Turun yliopisto
University of Turku

REMOTE SENSING FOR THREE-DIMENSIONAL MODELLING OF HYDROMORPHOLOGY

Claude Flener

TURUN YLIOPISTON JULKAISUJA – ANNALES UNIVERSITATIS TURKUENSIS
Sarja - ser. A II osa - tom. 302 | Biologica - Geographica - Geologica | Turku 2015

University of Turku

Faculty of Mathematics and Natural Sciences
Department of Geography and Geology
Geography Division

Supervised by

Adj. Prof. Petteri Alho, PhD
Department of Geography and Geology
University of Turku, Finland

Prof. Timo Huttula, PhD
Freshwater Centre
Finnish Environment Institute (SYKE), Finland

Reviewed by

Prof. David Gilvear, PhD
School of Geography, Earth and Environmental Sciences
Plymouth University
Plymouth, UK

Prof. James Brasington, PhD
School of Geography
Queen Mary University of London
London, UK

Opponent

Reader Robert Bryant, PhD
Department of Geography
The University of Sheffield
Sheffield, UK

The originality of this thesis has been checked in accordance with the University of Turku quality assurance system using the Turnitin OriginalityCheck service.

ISBN 978-951-29-6108-5 (PRINT)
ISBN 978-951-29-6109-2 (PDF)
ISSN 0082-6979
Kirjasitomo Kluutti Oy, Turku, Finland 2015

ABSTRACT

Flener, Claude
Remote sensing for three-dimensional modelling of hydromorphology

Successful management of rivers requires an understanding of the fluvial processes that govern them. This, in turn cannot be achieved without a means of quantifying their geomorphology and hydrology and the spatio-temporal interactions between them, that is, their hydromorphology. For a long time, it has been laborious and time-consuming to measure river topography, especially in the submerged part of the channel. The measurement of the flow field has been challenging as well, and hence, such measurements have long been sparse in natural environments. Technological advancements in the field of remote sensing in the recent years have opened up new possibilities for capturing synoptic information on river environments. This thesis presents new developments in fluvial remote sensing of both topography and water flow. A set of close-range remote sensing methods is employed to eventually construct a high-resolution unified empirical hydromorphological model, that is, river channel and floodplain topography and three-dimensional areal flow field.

Empirical as well as hydraulic theory-based optical remote sensing methods are tested and evaluated using normal colour aerial photographs and sonar calibration and reference measurements on a rocky-bed sub-Arctic river. The empirical optical bathymetry model is developed further by the introduction of a deep-water radiance parameter estimation algorithm that extends the field of application of the model to shallow streams. The effect of this parameter on the model is also assessed in a study of a sandy-bed sub-Arctic river using close-range high-resolution aerial photography, presenting one of the first examples of fluvial bathymetry modelling from unmanned aerial vehicles (UAV). Further close-range remote sensing methods are added to complete the topography integrating the river bed with the floodplain to create a seamless high-resolution topography. Boat- cart- and backpack-based mobile laser scanning (MLS) are used to measure the topography of the dry part of the channel at a high resolution and accuracy. Multitemporal MLS is evaluated along with UAV-based photogrammetry against terrestrial laser scanning reference data and merged with UAV-based bathymetry to create a two-year series of seamless digital terrain models. These allow the evaluation of the methodology for conducting high-resolution change analysis of the entire channel. The remote sensing based model of hydromorphology is completed by a new methodology for mapping the flow field in 3D. An acoustic Doppler current profiler (ADCP) is deployed on a remote-controlled boat with a survey-grade global navigation satellite system (GNSS) receiver, allowing the positioning of the areally sampled 3D flow vectors in 3D space as a point cloud and its interpolation into a 3D matrix allows a quantitative volumetric flow analysis. Multitemporal areal 3D flow field data show the evolution of the flow field during a snow-melt flood event. The combination of the underwater and dry topography with the flow field yields a compete model of river hydromorphology at the reach scale.

YHTEENVETO (FINNISH SUMMARY)

Flener, Claude
Kolmiulotteinen hydromorfologinen mallintaminen kaukokartoituksella

Jokien onnistunut hallinta edellyttää virtavesien prosessien ymmärtämistä. Tämä ei ole mahdollista ilman jokien geomorfologian ja hydrologian kvantifiointia sekä niiden spatiotemporaalisten suhteiden tutkimista, eli jokien hydromorfologiaa. Joen topografian mittaaminen, varsinkin uoman vedenalaisen osalle on pitkään ollut työlästä ja aikaa vievää. Virtauskentän kattava mittaaminen on myös ollut haastavaa, sillä seurauksella, että niitä on tehty harvakseltaan luonnollisessa ympäristössä. Viimeaikainen teknologinen kehitys kaukokartoituksessa on mahdollistanut synoptisen tiedon mittaamisen jokiympäristöissä. Tässä väitöstutkimuksessa on kehitetty virtavesien kaukokartoitusta sekä jokien topografian että virtausmittauksen alalla. Useita eri lähikaukokartoitusmenetelmiä yhdistämällä on tehty korkean resoluution yhtenäinen empiirinen malli joen hydromorfologiasta, eli joen uoman ja tulvatasangon topografiasta ja kolmiulotteisesta virtaamakentästä.

Empiriaan ja hydrauliseen teoriaan perustuvat optisen kaukokartoituksen menetelmiä testattiin ja arvioitiin käyttämällä normaaliväri-ilmakuvia, kaikuluotain kalibrointia ja referenssimittauksia kivipohjaisessa subarktisessa joessa. Empiiristä optista syvyysmallia kehitettiin edelleen lisäämällä syvän veden säteilyparametrin arviointialgoritmi, joka mahdollisti mallin käytön myös matalavetisissä jokiuomissa. Parametrin vaikutus malliin arvioitiin korkean resoluution matalailmakuvista hiekkapohjaisessa subarktisessa joessa yhdessä ensimmäisistä syvyysmalleista, joka on tehty käyttäen kauko-ohjattua minihelikopteria (*eng.* UAV, Unmanned Aerial Vehicle). Lähietäisyyden kaukokartoitusmenetelmiä käytettiin edelleen topografisen mallin täydentämiseen, integroimalla joen uoma ja tulvatasanko yhtenäiseksi korkean resoluution topografiaksi. Mobiilia laserkeilausta käytettiin vedenpinnan yläpuolisen osan topografian mittaamiseen korkealla resoluutiolla vene- kärry- ja reppupohjaisten kartoitusalustojen avulla. Monen ajankohdan mobiilin laserkeilauksen ja UAV-fotogrammetrian tarkkuutta arvioitiin maalaserikeilausaineiston avulla. Laserkeilattu ja fotogrammetrinen aineisto yhdistettiin, jolloin saatiin kahden vuoden ajalta saumaton digitaalinen maastomalli. Mallin avulla oli mahdollista arvioida koko joen uoman korkean resoluution muutosanalyysin metodologiaa. Kaukokartoitukseen perustuvaa hydromorfologista mallia täydennettiin uniikilla virtauskentän kolmiulotteisella kartoitusaineistolla. Kauko-ohjattavaan veneeseen asennettu akustinen virtausmittauslaite yhdessä tarkan satelliittipaikannusjärjestelmän kanssa mahdollistivat alueellisesti valikoitujen kolmiulotteisten virtausvektoreiden sijainnin määrittämisen kolmiulotteisessa avaruudessa pistepilvenä. Tämän aineiston kolmiulotteinen interpolaatio matriisiksi mahdollisti edelleen volymetrisen virtausanalyysin. Monen ajankohdan alueellinen kolmiulotteinen virtauskenttä osoitti virtausolosuhteiden evoluution kevättulvassa. Vedenalaisen ja kuivan maan topografia yhdessä jokiuoman virtauskenttien kanssa muodosti kattavan mallin joen hydromorfologiasta.

ACKNOWLEDGEMENTS

This doctoral dissertation is based on my work at the Fluvial Research Group at the Division of Geography at the University of Turku during the years 2010 – 2014. The work was carried out in collaboration with the Department of Real Estate, Planning and Geoinformatics at Aalto University and the Department of Remote Sensing and Photogrammetry at the Finnish Geodetic Institute and the Freshwater Centre at the Finnish Environment Institute. This work has offered me many opportunities and experiences that I would have never gotten otherwise. I was able to work in some amazing places and meet many great people. I have learnt a lot from these valuable experiences.

First off, I would like to thank my supervisors Adj. Prof. Petteri Alho and Prof. Timo Huttula for their guidance and support of this work. Pete, without you, this thesis would not have happened. I am grateful for the opportunity, the support and the funding that you have provided during all these years.

Special thanks go to members of the Fluvial Research Group, past and present: Petteri Alho, Eliisa Lotsari, Elina Kasvi, Yunsheng Wang, Jenni-Mari Vesakoski, Leena Laamanen. Thanks for all the years we spent together in the field, in the office, on conference travels and in the pub. I have enjoyed working together with you guys. Thanks for many interesting conversations and encouragements. In particular, thanks to my long-time roomies Eliisa and Elina. It has been great working with you for all that time.

Many thanks to my co-authors from outside the Fluvial Research Group: Matti Vaaja, Anttoni Jaakkola, Harri Kaartinen, Antero Kukko, Anssi Krooks, Matti Kurkela, Juha Hyyppä, Harri Hyyppä and Jukka Käyhkö. Your contribution has been crucial to this thesis. It has been very enjoyable working with you and it is amazing to have a team with such great and diverse expertise to work with. Most of this work would not have been possible without you. In addition to the "Pulmanki Crew" of many years, Pete, Eliisa, Elina, Antero, Harri, Matti, Matti, Anttoni, Leena, Yunsheng, thanks also belong to other field work collaborators and assistants: Saija Koljonen, Lauri Harilainen, Laura Lehtiö, Sudhir Karki, Mikel Calle Navarro, Kristiina Hakala, Tuuli-Anna Raippalinna, Maria Kämäri. Thanks also to the personnel of the Kevo Subarctic Research Institute and the Tana river station of the Game and Fisheries Research Institute for their support during our field work campaigns.

Then, I would like to thank Prof. David Gilvear and Prof James Brasington for reviewing the manuscript of this thesis and for their encouraging comments.

Many thanks also to my colleagues at the division of Geography who have contributed to my work in any possible way, in particular Risto, Annukka, Leena, Joni and Kirsi. Thanks also belong to the Pasi Saaremaa and his team at the "Fyysikan paja". I wish to also thank the Doctoral programme in Biology, Geography and Geology for providing funding for part of this work.

Finally, I want to specially thank my parents Roger and Mariette, and my sister Martine and her family for their encouragement and support. Thanks also to my friends and family for their support during this thesis. And last, but by no means least, very special thanks to Hanna for her love and understanding and encouragement during all these years.

LIST OF ORIGINAL PAPERS

This thesis consists of a summary and the following four original papers. The papers are referenced by their roman numerals.

I Flener, C., Lotsari, E., Alho, P., and Käyhkö, J., 2012: Comparison of empirical and theoretical remote sensing based bathymetry models in river environments. *River Research and Applications*, 288–133, doi: 10.1002/rra.1441.

II Flener, C., 2013: Estimating deep water radiance in shallow water: adapting optical bathymetry modelling to shallow river environments. *Boreal Environment Research*, 18, 488-—502.

III Flener, C., Vaaja, M., Jaakkola, A., Krooks, A., Kaartinen, H., Kukko, A., Kasvi, E., Hyyppä, H., Hyyppä, J., and Alho, P., 2013: Seamless Mapping of River Channels at High Resolution Using Mobile LiDAR and UAV-Photography. *Remote Sensing*, 5, 6382-–6407, doi: 10.3390/rs5126382.

IV Flener, C., Wang, Y., Laamanen, L., Kasvi, E., Vesakoski, J.-M., and Alho, P., 2015: Empirical modelling of spatial 3D flow characteristics using a remote-controlled ADCP system – monitoring a spring flood. *Water*, 7, 217–247, doi: 10.3390/w7010217.

CONTENTS

1 INTRODUCTION

Rivers are one of the main agents in shaping our landscapes. They connect the land to the sea as a conduit of not just water but with it a slew of physical and chemical particles. Rivers are also ecologically important by providing important in-channel and riparian habitats. In recent decades, river management and restoration has gained increasing importance (Shields and Rigby, 2005; Koljonen, 2011).

Successful management of rivers requires on the one hand an understanding of the basic processes that govern them, that is, how the water flow affects topography and vice-versa and on the other hand, a means of quantifying these processes and their effects, that is, their hydromorphology (Vaughan et al., 2009).

The European Commission (2000) places hydromorphology as a central aspect of the Water Framework Directive that aims at protecting and enhancing aquatic ecosystems throughout the European Union. "Hydromorphology describes the geomorphology and hydrology of a river system, their interactions, and their arrangement and variability in space and time" (Vaughan et al., 2009). This includes the spatio-temporal aspects of river channel and flood plains, their geomorphology, connectivity, sediment processes, hydrology, as well as engineering measures and human impacts. In this thesis, the hydromorphology is defined to encompass the geomorphology of the river, that is, the shape of the river channel and the floodplain, and the flow field, that is, the "shape" of the water current flowing over the topography. The successful management of such a complex system, taking an integrated approach, requires information that goes beyond what can be measured as local samples in the field (Gilvear et al., 2004). Modern remote sensing methods allow to gain a synoptic view of river environments (*e.g.* Lane et al., 2003; Legleiter et al., 2004) channel topography, water flow and riparian topography and land cover.

This thesis focuses on methods of quantifying hydromorphological elements: in particular, the spatial aspect and integration of mapping topography and flow is investigated. Rivers have long been studied and modelled in a segmented fashion. A real understanding of river environments requires a unified approach to how rivers are characterised and modelled (Carbonneau et al., 2012). Good quality, high resolution data is important to support modern investigations of river morphology, hydrology and habitats that often make use of computational models to both advance

the understanding of these systems and to predict their evolution or behaviour. The underwater realm is the most challenging to measure, but at the same time also the most geomorphologically active (Smith et al., 2012) and hydromorphologically relevant (Horritt et al., 2006).

Many hydraulic and hydrodynamic modelling applications require boundary conditions in terms of topography, discharge, water levels, slope and channel roughness (Bates et al., 2005). The lower order numerical flow models have low data requirements for their calibration. In recent years the use of higher order models has increased (*e.g.* Virtanen et al., 1994; Lane et al., 1999). These models are increasingly demanding of high quality and high resolution calibration data. This is one reason why three-dimensional (3D) hydrodynamic models have thus far mostly been used in laboratories with field applications in rivers now slowly becoming more common (*e.g.* Kasvi et al., 2014). Meeting the data requirements for these models in natural streams has been extremely challenging. Anderson et al. (2001) noted that it is important to validate hydraulic models with measured data that can capture the complexity of real world flows and lamented the lack of availability of suitable data for the purpose.

Most measurement and modelling methodologies in river environments have been developed to address one specific aspect of hydromorphology and these methods have often been applied to study for instance geomorphology (*e.g.* Lorang et al., 2005; Heritage and Milan, 2009; Smith and Pain, 2009; Alho et al., 2011b; Javernick et al., 2014), ecology (*e.g.* Schmidtlein, 2005; Kondolf et al., 2006; Hill et al., 2008) or hydrology (*e.g.* Hardy et al., 1999; Horritt et al., 2006; Bates, 2004). Recently, combinations of methodologies have been applied to study more complex integrated dynamics of rivers (*e.g.* Wheaton et al., 2010; Carbonneau et al., 2012; Fuller and Basher, 2013). Carbonneau and Piégay (2012) argue that "localised, non-continuous, sampling of small scale river processes, forms and biota leads to a fundamental scale mismatch between the processes under scrutiny and our data collection."

The present work contributes to mapping natural river environments by presenting a combination of methods for quantifying river environments at high resolution in a unified, spatially continuous way, that is, the measurement and modelling of river bathymetry merged with flood plain topography and adding the water flow into this riverine landscape. River science and management can be moved forward by this unified modelling approach that provides an empirical model of an actually measured situation, rather than a computational model based on hydraulic theory and a range of assumptions.

1.1 Aim and objectives

The aim of this thesis is to advance remote sensing in hydromorphology by developing a framework for creating a unified river model of seamless fluvial topography and water flow field. In order to fulfil this aim, empirical and theoretical modelling approaches for image-based remote sensing of river bathymetry are evaluated. A new deep-water correction parameter estimation method is presented and evaluated. This method is applied together with state-of-the-art mobile, high-resolution map-

ping technologies to create a seamless model of riparian and channel topography, i.e. fluvial topography. This methodology is presented and evaluated for its suitability for inter-annual change detection. The flow element is added to the integrated model in the form of a multi-dimensional flow-field modelling methodology. The models are implemented and tested on two sub-Arctic rivers, one gravel-bed and one sand-bed stream.

The specific objectives of this thesis are:

- to compare different optical models for modelling bathymetry in shallow rivers.
- to assess the sensitivity of the deep water correction parameter in Lyzenga's (1981) linear transform model.
- to benchmark different survey methods for fluvial topography modelling.
- to assess the feasibility of creating seamless wet-dry topography models.
- to develop a methodology for surveying three-dimensional river flow fields.
- to build a complete 3D model of river environments including dry and submerged topography and the flow of water.

Paper I focuses on the submerged channel form and presents a comparison of different methods for remote sensing of river bathymetry based on aerial imagery. Specifically, two models based on hydraulic theory that present an interesting and novel approach to bathymetric modelling are compared to an empirically based model transposed from marine environments that requires ground data for its calibration. This was the first test of the theoretical models outside of their development site. The empirical model came favourably out of the analysis.

Paper II focuses on a specific parameter of the empirical bathymetric model used in I, deep water radiance, that had thus far been largely ignored in bathymetric modelling in rivers due to the difficulty in parametrizing it. An algorithm for estimating deep water radiance is presented and used to analyse under which circumstances this parameter is important or whether it can safely be ignored in modelling river bathymetry.

Paper III widens the scope of remote sensing of river topography to include the flood plain as well as the submerged river bed. A new method is presented for combining high resolution mobile laser scanning techniques with UAV-based aerial photography that is used with photogrammetry to create a model of topography as well as orthoimagery, that in turn is used to create a bathymetry model by applying the methods developed further in I and II. The combination of these techniques results in a seamless topography model representing wet and dry topography at the reach scale at unprecedented resolution. A two-year time series of this seamless model is used for conducting a change analysis.

Paper IV represents the next step to a complete empirical river environment model by adding the water itself onto this seamless topography. A novel measuring and modelling methodology is presented that combines ADCP measurements with high-accuracy global navigation satellite system (GNSS) positioning deployed from a remote-controlled boat. The raw ADCP data is processed together with the GNSS data to form a 3D point cloud of flow vectors giving a new perspective of the 3D flow field measured in a real river.

The present work combines the outcomes of these papers into one complete concept and a set of methods that allow creating a comprehensive empirical model of river environments based on real measured data: a model of the river topography

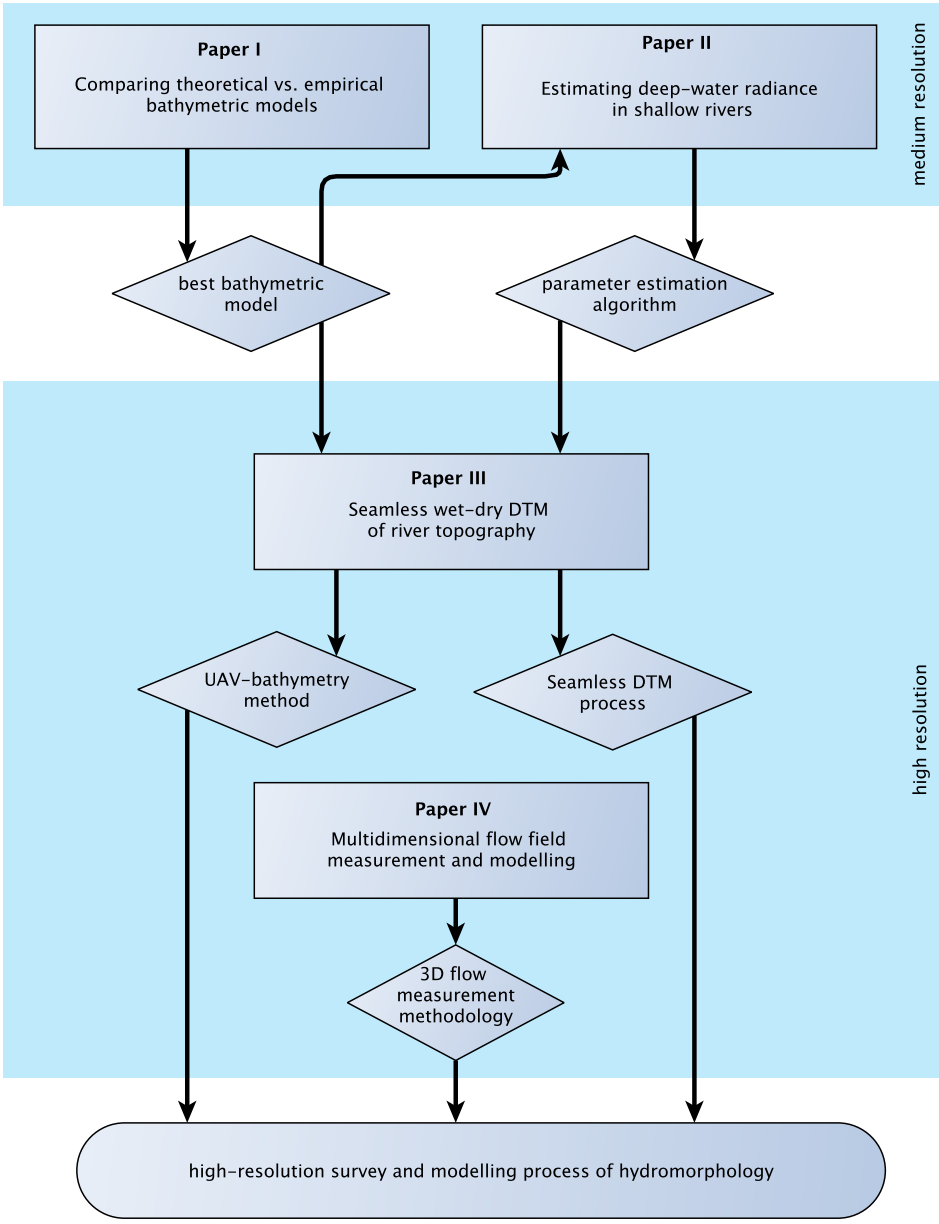

FIGURE 1 Flow chart of the study approach of the thesis. The rectangular boxes illustrate the main aim of each included article. The rhombuses contain the main outcome of the corresponding article. The arrows indicate how the outcomes of earlier articles provide input methodologies for later work. The oval is the combination of the outcomes of all the articles into a unified model of hydromorphology. The background shows the progress from the medium resolution aerial photography to the high resolution provided by the close-range remote sensing methods used in the later articles.

including the submerged river bed and the flood plain, and then the water flow can be "poured" over this topography to complete the model of the river environment.

2 SURVEYING RIVERS

The comprehensive view of river environments inherent in the concept of hydromorphology viewing rivers as holistic systems leads to the requirement of spatially continuous data. This requirement is best fulfilled by remote sensing methodologies (Carbonneau and Piégay, 2012). Gilvear et al. (2004) reasoned that "remotely sensed imagery can give the synoptic view that allows panoptic mapping of river hydromorphology and human impacts". In fact, a substantial body of research on remote sensing specifically in river environments has been compiled in recent years, leading Marcus and Fonstad (2010) to coin the term 'Fluvial Remote Sensing' in recognition of the fact that remote sensing in fluvial research has emerged as a self-contained sub-discipline of remote sensing. The following sections give an introduction to fluvial processes, creating a context for the measurements undertaken in the original papers of this thesis, and introduce the backgrounds to the range of measurement and surveying methods employed in this work.

2.1 Background on remote sensing in river environments

Remote sensing can be defined to encompass any method of acquiring information about a physical characteristic or phenomenon without directly measuring it by means of touch. (*e.g.* Lillesand et al., 2008). Among the multitude of means to gather information remotely, in river environments, the most commonly used include aerial images, including multispectral imagery, as well as Radar and more recently, LiDAR (Light detection and ranging). Satellite images, as well as data of other satellite-borne sensors, have long had too coarse a resolution to map anything but the largest streams (*e.g.* Mertes et al., 1993; Papa et al., 2007; Birkinshaw et al., 2010) and have therefore found fairly little use in most river research, although recently finer resolution satellite data has been successfully used in river environments (*e.g.* Legleiter and Overstreet, 2012).

When taking a broad view on remote sensing, measuring the depth of water by means of an echo-sounder or sonar is also remote sensing (Carbonneau and Pié-

gay, 2012). Extending that concept, it can be argued that measuring flow by acoustic means using an acoustic Doppler current profiler (ADCP) is also a form of remote sensing. Indeed, in this work, the term is considered broadly enough to encompass acoustic flow measurement as remote sensing of flow characteristics, in contrast to direct flow measurement by propeller-based flow meter for instance.

The following sections outline a diversity of remote sensing techniques relating to river environments, touching on the parameters to be measured as well as the methods that can be employed to this end. It is the sub-discipline of Fluvial Remote Sensing that this thesis tries to make a contribution to, as well as push the boundary of the concept a little, by including the remote sensing of water flow.

Fluvial remote sensing can encompass any aspect of hydromorphology including the active channel, that is the part of the channel that is submerged at low flow and the unvegetated flood plain, as well as other riparian areas and their topography and land cover. The focus here is mainly on the active channel and, to a smaller degree, the immediate riparian area. Further aspects that may be considered part of hydromorphology that may be investigated by remote sensing, such as entire catchment topography or land use are not covered here.

Optical imagery is by far the most commonly used means of remote sensing in rives. Airborne imagery has found applications for mapping flood extents (*e.g.* Smith, 1997; Bates et al., 1997; Brakenridge et al., 2005), in-stream habitats including submerged vegetation (*e.g.* Wright et al., 2000; Marcus, 2002; Legleiter, 2003; Cho and Lu, 2010), suspended sediment and turbidity (*e.g.* Mertes et al., 1993; Dekker et al., 1997; Mertes, 2002) as well bed sediment (*e.g.* Lyon et al., 1992; Castillo et al., 2011). High-resolution aerial photography has been used to map grain sizes in gravel bed rivers successfully (*e.g.* Carbonneau et al., 2004; Castillo et al., 2011) including shallow wetted areas (Carbonneau et al., 2005). Grain sizes and bed roughness have also been successfully extracted using terrestrial laser scanning (*e.g.* Entwistle and Fuller, 2009; Heritage and Milan, 2009) and mobile laser scanning (Wang et al., 2013).

Arguably the most commonly mapped parameter in rivers is water depth. The remote sensing of bathymetry in rivers is one of the main aspects of this work and is dealt with in detail in Section 2.3 in particular with respect to optical imagery, as well as sonar and LiDAR.

River research requires different data depending on its focus and scale. Data required in catchment hydrology research are generally mainly large scale digital elevation models (DEM) and coarse hydrological data, such as precipitation and a river hydrograph. Traditionally, such data were acquired using non-remote surveying techniques such as tacheometry. Remote sensing makes it possible to gather data over large areas rapidly. In river research, remote sensing is predominantly used to acquire topography data, but remote sensing is also widely used for land cover classification, monitoring of vegetation cover and phenology, ground water monitoring, meteorological monitoring, snow cover monitoring or mapping the extent of glaciers or sea ice in the Arctic, to name but a few applications. Indeed, mapping land use can be of great use in river research, in particular in relation to flood research.

The spatial resolution of these data varies greatly, depending on the sensors used. Typical resolutions can vary from 30 m for Landsat satellite data to a few cm in the case of close-range remote sensing from low-flying aircraft or ground-based mobile mapping systems. The ability to cover large areas rapidly brings about data at unprecedented densities and time intervals that make whole new angles of enquiry

possible. One obvious and often applied research topic is change analysis of environments. With rivers, change analysis can take many forms, focusing on catchment scale hydrology or reach scale geomorphology (*e.g.* Kasvi et al., 2013) or on habitat distribution (*e.g.* Wheaton et al., 2010), for instance. One particular aspect that remote sensing has been mostly employed for is mapping topography. In the context of rivers, topography is important in a basic way in which it shapes the river system, and conversely, how the river system changes topography.

2.2 Fluvial processes — Measuring the flow of water

2.2.1 Short introduction to fluvial processes

The flow of water is the essence of a river. It shapes the river while the shape of the river directs the flow. This dynamic process has long been studied and the fundamental relationships governing flow were established decades ago (*e.g.* Leopold and Wolman, 1960) based on even earlier experimental foundations (*e.g.* Reynolds, 1883). This section gives a short overview of the processes at play to set the context for the measuring and modelling conducted in this thesis. A detailed review of the complex hydraulics of open channel flow is beyond the scope of this work.

Water flowing in an open channel is driven by gravity and slowed by friction at the channel boundary and causes sediment transport. The potential energy of the mass of water at higher elevation is converted to kinetic energy as it flows downhill, manifested as velocity, dissipated by turbulence and exerting force on the channel boundary (Wohl, 2014). Flow can be uniform, with constant velocity independent of position, or non-uniform, with spatially varying velocity. Flow with velocity that stays constant throughout time is said to be steady (Figure 2 a.i), whereas velocity variation through time gives unsteady flow (Figure 2 a.ii). Flow can also be either laminar (Figure 2 b.i), that is, all water is moving in the same direction without mixing, or turbulent (Figure 2 b.ii), with irregular and sporadic flow paths and momentum transfer by eddies. The level of turbulence is often quantified by the Reynolds number (Re), a dimensionless number that quantifies the ratio of the inertial forces of the flow (flow velocity v (ms^{-1}), hydraulic radius R (cross-sectional area / wetted perimeter), and water density ρ ($\mathrm{kg\,m}^3$)) to the molecular viscosity of the water μ (Knighton, 1998):

$$\mathrm{Re} = \frac{vR\rho}{\mu} \tag{1}$$

Flow in natural channels is generally non-uniform, unsteady and turbulent, with a small slow-moving laminar sub-layer near the channel boundary, *i.e.* the river bed. Furthermore flow can be tranquil or rapid, quantified by the dimensionless Froude number (Fr), defining subcritical (Fr<1), critical (Fr=1), or supercritical (Fr>1) flow, expressing the ratio of flow inertia to gravitational forces:

$$\mathrm{Fr} = \frac{v}{\sqrt{g\frac{a}{w}}} \tag{2}$$

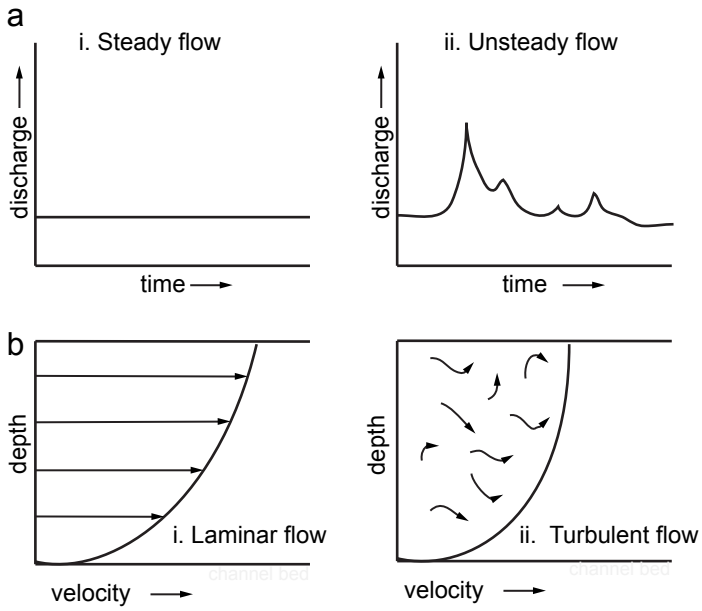

FIGURE 2 Types of flow in open channels: (a) steady *vs.* unsteady flow, (b) laminar *vs.* turbulent, adapted from Knighton (1998).

where g is gravitational acceleration (ms^{-2}), a is the cross-sectional area normal to the direction of flow (m^2), and w is the free surface width (m) (Chow, 1959).

Flow velocity and volume, *i.e.* discharge, are the most important hydraulic variables. Discharge Q (m^3s^{-1}) is a function of channel width w (m), depth d (m) for a given cross-section and mean velocity v (ms^{-1}) expressed as the flow continuity equation:

$$Q = wdv \tag{3}$$

The width and depth of the channel are influenced by slope and substrate, which in turn affect velocity, and thereby, energy exerted on the channel boundary. The shape of the channel and frictional resistance of its substrate determine how much energy is expended and how much sediment is potentially transported. Sediment transport is influenced by sediment type and availability as well as flow properties such as velocity, viscosity and turbulence which influence frictional forces on the channel boundaries.

Eddies help to carry dissolved particulate matter in the water column and disperse it throughout the flow field. Eddies dissipate flow energy due to both internal friction from viscosity (Chow, 1959) and due to eddy viscosity as the horizontal and vertical transfer of momentum in the flow by turbulent mixing (Robert et al., 2003). The work the flow exerts on the channel boundary, that is the rate of energy dissipation from the water to the river bed, is known as stream power (Wm^{-1}), which can be quantified either as total stream power (Bagnold, 1966):

$$SP = \rho gQS \tag{4}$$

where S is slope, or as the spatially variable unit stream power ω (Bull, 1979):

$$\omega = \rho gdSv \tag{5}$$

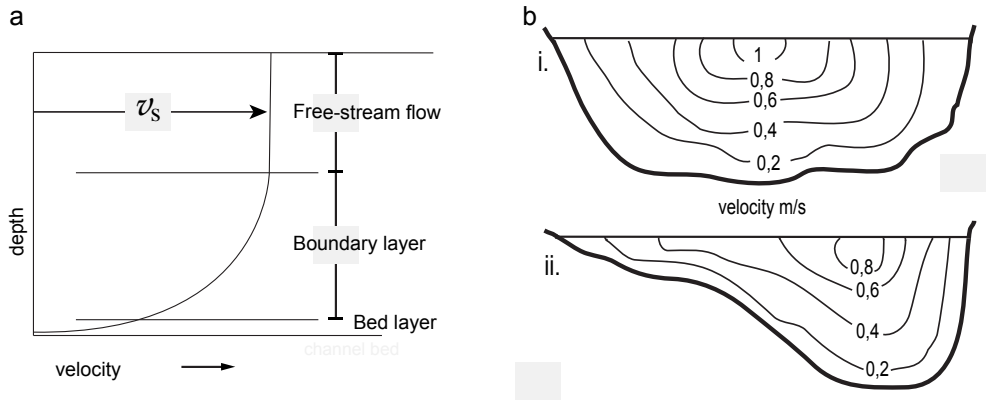

FIGURE 3 (a) The different flow layers representing the frictional effect of the boundary on the flow. Free-stream flow does not occur in shallow water; (b) velocity variability with distance from boundary and across the stream in natural channels, adapted from Knighton (1998)

Unit stream power, in particular can be used together with bed shear stress (Nm^{-2}), that is the resistance of the river bed to flow forces, which is essentially unit stream power without considering velocity, as a way to quantify the spatial interaction of flow and river bed, which is related to sediment transport (*e.g.* Kasvi et al., 2013; Lotsari et al., 2014).

Flow velocity — along with accurate positional data for slope and depth — is therefore an essential variable to measure in order to study the dynamics of hydraulics and river bed geometry and resistance. Flow patterns vary over time and space, particularly when considering three-dimensional flow and an understanding of turbulence and velocity is important because of its dynamics relating to channel morphology and sediment transport (Leeder, 1983; Wohl, 2014). In particular, flow varies with distance from the boundary (Figure 3 a), and across the stream (Figure 3 b) and with time (Knighton, 1998).

There is a large variety of natural channel forms that are rarely straight with symmetrical cross-sections, but rather meandering or braided, which leads to more complexity in flow patterns, which, in turn, leads to a complex spatial distribution of erosional and depositional forces. These complexities and their implications on river geomorphology as well as changes to these patterns with changing discharges have long been recognised (*e.g.* Leopold, 1953; Leopold and Wolman, 1960; Dietrich and Smith, 1983). For instance, the flow in a meander bend, which usually consists of a gently sloping point bar on the convex side and deep pool with a steep rise to the concave shore (Leopold and Wolman, 1960) does not follow the same flow field distribution of a straight channel that can be simplified as an exponentially increasing velocity with increasing distance form the channel boundary (Knighton, 1998) (Figure 3). The curved shape of a river bend introduces a three-dimensional flow field with the high velocity core (HVC) located near the inner bank, shifting gradually outwards towards the apex of the bend (Leopold and Wolman, 1960; Dietrich and Smith, 1983), causing a super-elevation of the water surface on the concave side of the bend, forcing the water to move downwards, which leads to an overturning motion in the downstream direction with the flow eventually rising towards the inner bank

(*e.g.* Bathurst et al., 1979). The flow field, needs to be considered in a three-dimensional manner and can be characterised at any instant in time as a 3D field of velocity vectors, each being a quantity with a magnitude and direction in three dimensions, and a position in 3D space (*e.g.* Fox, 1978; Wohl, 2014). The methodology presented in Paper IV opens new possibilities of characterising these variables in natural river environments.

2.2.2 Background on flow measurement

The flow of liquids or gases can be measured in a variety of ways and for a variety of purposes. The focus here is strictly on measuring open channel flow, so any methods and applications relating to flow in pipes for example are not considered in this section.

2.2.2.1 Measuring discharge

Open channel flow is measured most often for the purposes of determining discharge. For this, a cross-section or transect of a river is chosen at a location with ideally uniform flow conditions, that is, in a straight section of river, preferably without obstructions upstream for a distance of about five times width. The cross-section is divided into vertical sections in which flow velocity is measured at one or several depths, depending on depth, traditionally using a mechanical or electromagnetic current meter. The average depth of each vertical section is recorded so that its area can be calculated. This cross-sectional area times the flow velocity adjusted for measurement depth gives an estimate of discharge at that vertical section. The sum of all the vertical sections in a cross-section totals the discharge as a measure of volume of water per unit time passing that cross-section according to Equation 3 (WMO, 2008). Generally, discharge is measured in m^3s^{-1} but managers may use other measures, particularly in smaller streams, where litres per minute or m^3 per day may be more useful units of measure.

Another method to calculate discharge is by pouring a chemical tracer into the stream and measuring its concentration further downstream after the tracer is fully mixed with the water. The dilution of the tracer is proportional to discharge. While this method can be very useful for measuring discharge in certain circumstances, such as strongly turbulent, shallow, rocky mountain rivers with near critical or supercritical flow where flow measurement would be very difficult, the tracer method only gives discharge, but no flow data.

A non-contact method for measuring discharge involves a Doppler radar that measures surface velocity, as pioneered by Costa et al. (2000). Sommer Messtechnik ltd. has developed a stationary instrument based on this principle consisting of one vertically downward looking radar sensor and one Doppler radar sensor mounted at a 45° angle to the vertical. The instrument is mounted in a fixed position above the water surface, for instance on a bridge, and measures its distance to the water surface to determine stage using the ranging radar and based on the Doppler shift (more on this in Section 2.2.2.2) of the returned radar signal scattered from moving ripples on the water surface, the water surface velocity is determined. A calibrated algorithm based on hydraulic theory estimates discharge from the measured stage and surface velocity, combined with an input cross-sectional profile. While this method involves

truly remotely sensed discharge and surface flow data in the sense that the sensor is not in contact with the water, it is beyond the scope of this work.

2.2.2.2 Flow meters

Traditionally, flow was measured using a mechanical or electromagnetic flow meter (*e.g.* Leopold, 1953; Bathurst et al., 1979). Mechanical flow meters or current meters consist of an propeller mounted to a pole and connected to a counter that records the number of revolutions of the propeller. The device is put into the flowing water pointing upstream and velocity is recorded by counting the number of revolutions of the propeller in a given amount of time, often 50 seconds. The distance of one revolution is a known constant and the increase in propeller speed is linear to flow velocity, so flow velocity can be determined in ms^{-1}. Electromagnetic flow meters measure current in the form of a voltage created by water flowing through a magnetic field created by the measurement device that is deployed in the same manner as a propeller based flow meter. Some electromagnetic flow meters are able to measure two perpendicular components of flow simultaneously (Bathurst et al., 1979).

The relatively long sampling time that these meters integrate the flow over into one measurement ensures that the measurement is representative of the average flow velocity at the measurement position. This time integration filters out small-scale eddies and turbulence. This is an important consideration in flow measurements that is discussed further in Paper IV. Muste et al. (2004a) have analysed the effect on sampling time with respect to stationary ADCP measurements, but the same principle applies to all stationary flow measurements. Some advanced versions of propeller flow meters include a computer that helps in recording station depths, measurement depths, and flow velocities and computes discharge based on these input data.

A more modern method for measuring water currents is the acoustic Doppler velocimeter (ADV) developed in the early 1990's (Kraus et al., 1994). This device is an evolution on the computer assisted propeller system: rather than an propeller that directly converts flow into a measure of distance, the ADV uses an acoustic pulse and two or three receiver sensors mounted at an angle so they focus at a short distance away from the transducer. The sensors simultaneously record the acoustic scatter returned from particles in the flowing water (*i.e.* suspended sediment, suspended debris, zooplankton) and based on the phase change caused by the Doppler shift of these return signals, both the velocity and the direction of the flow can be determined, in 2D horizontally or in 3D including vertical flow angle, depending on the number of receivers (Rehmel, 2007).

Given that the geometry of the transducer and receivers is known, and the Doppler effect that causes sound waves to shift towards longer wavelengths when they are reflected off an object moving away from the sensor and towards shorter wavelengths when the scatterer is moving towards the sensor, two opposing sensors recording the return of the same emitted signal give enough data to compute the direction the scatterer was moving in relative to the sensors and, based on the magnitude of the Doppler shift, the velocity as well.

Analogously to the propeller system, the ADV also measures stationary flow for a period of time, generally measuring one data point per second that are then averaged into one flow vector over that given period of time. Strictly speaking this is remote sensing of flow velocity, because, unlike the propeller, the sensors are not

in contact with the water that is actually being measured. The focal point of the sensors is generally about 10 cm away from the transducer that emits the sound waves. Considering that this method of measuring flow velocity involves submerging the sensor into the flow to be measured, most would not consider this method to constitute remote sensing. It is worth noting, however, that this method is an indirect measurement of flow, because what is really being measured is the motion of scattering particles in the water that are assumed to move at the same speed as the water itself. This also represents a limitation of the system, since the flow of clear water with no suspended particles at all can not be measured acoustically.

Lane et al. (1998) used a downward-looking ADV to map 3D flow velocities in a small stream and compared the measurements of the then new device to the better known electromagnetic current meter and found the ADV to perform well. propeller-based and electromagnetic flow meters and ADVs have the advantage that they are able to measure flow even in very small streams, as long as the sensor or propeller can be fully submerged. These measurement methods have the downside of being very slow, and somewhat limited or complicated to apply in deep water. On larger rivers or in strong currents, these measurement methods are potentially hazardous. The current meters are often deployed manually from a platform tethered in position to a steel cable stretched across the stream. This has led to accidents involving other boats not seeing the cable or the measurement platform capsizing in strong currents ending fatally for the surveyors.

2.2.3 Acoustic Doppler Current Profilers

Another variation on the principle of acoustic Doppler velocity measurement lead to the creation of the acoustic Doppler current profiler (ADCP). ADCPs were originally developed by RD Instruments and have been commercially available since the 1980's (*e.g.* Gordon, 1989). Although ADCPs are available in a variety of set-ups, such as horizontal (*e.g.* Nihei and Kimizu, 2008; Hoitink et al., 2009) or vertically upwards facing systems (Fitzpatrick, 2011), the discussion here focuses on mobile, downwards-looking ADCP systems only.

Early ADCPs required fairly deep water to operate in, so they were used in marine environments before it was possible to use them in shallower rivers. Simpson et al. (1990) for instance used an ADCP to map the flow field in the channel separating the outer Hebrides form mainland Scotland. Here, flow is measured based on the same effect of the Doppler shift of sound waves returning to a sensor from a scatterer in the water column, but rather than the sensors focusing on one small area of water near the transducer, a set of usually three or four transducers is arranged at an angle, usually between 20° and 30° from the vertical, facing away from each other (Figure 4). A sound beam with a frequency of up to several MHz is emitted from each transducer and the returned signals are picked up from different directions surrounding the instrument. Assuming the ADCP to be stationary and flow to be homogeneous, that is, not to contain eddies or turbulence, the combination of the Doppler shifts registered in all directions makes it possible to determine the average direction and velocity of flow under the ADCP (*e.g.* Yorke and Oberg, 2002; Muste et al., 2004b; Gunawan et al., 2011). Horizontal flow can be calculated based on three sensors, and a fourth one allows to determine the vertical component of the flow vector as well.

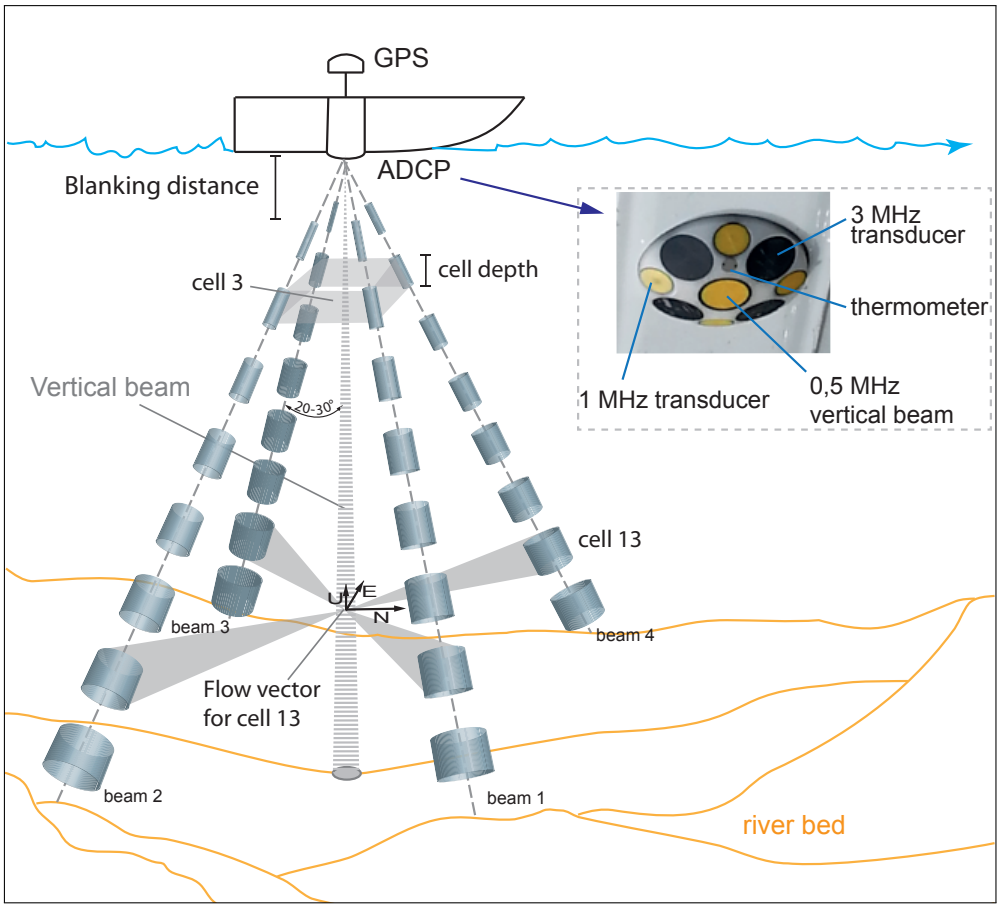

FIGURE 4 Illustration of the operating principle and geometry of a four-beam downward-looking ADCP. The four acoustic Doppler beams are illustrated, showing every other measurement cell in each beam. Cell 3 indicates the volume of water that conceptually forms the cell, vs. how the individual beam measurements relate to the measured vector ENU that is conceptually located directly underneath the sensor, as illustrated for cell 13. The pyramid shaped arrangement of the cells with the distance between beams increasing with depth can be seen (pyramid angles are exaggerated), along with the vertical beam for depth sounding, the blanking distance and an image showing the arrangement of the transducers on the Sontek M9.

It has to be considered that the flow vector that is calculated is conceptually located underneath the ADCP, whereas the device measures return signals from around the sensor, not directly underneath it (*cf.* Figure 4), or above it, in case of an upward looking system. The sensor configuration makes it possible not only to determine the flow velocity for each beam based on the Doppler shift, but to also to determine distance based on the return time. ADCPs generally split the water column vertically into layers, so that a flow vector is calculated for each depth layer separately. These vertically split velocity vectors are called cells or bins. One measurement consisting of a stack of cells is called a sample or ensemble. As described above, and ADCP integrates the signals of three or four beams into one vector containing information on

flow velocity and direction at different depths, often expressed as Eastwards, Northwards, and Up velocity components (ENU). A stationary measurement of this sensor with similar duration as an ADV will give an accurate flow measurement at that point (Muste et al., 2004a).

ADCPs can be configured in a range of different ways when deployed in a stationary manner. They can be mounted on a mooring platform looking downward, or sideways looking mounted on an embankment or an engineering structure in a channel. There are also upward looking ADCPs designed to monitor the discharge in irrigation ditches.

One major advantage ADCPs have brought over other methods of measuring flow and/or discharge, is that they can be deployed form a moving platform. This allows measuring flow in a spatial manner. Initially, and still most commonly, mobile ADCPs are used to measure transects either for flow field mapping (*e.g.* Dinehart and Burau, 2005a; Jamieson et al., 2011; Parsons et al., 2013; Petrie et al., 2013) or, more commonly for discharge measurement (*e.g.* Yorke and Oberg, 2002; Shields et al., 2003). In order for the ADCP to be able to compute flow velocity and direction of the water it needs to know its own movement, so that this can be compensated for in the flow calculation. There are several ways that the instrument can figure out its own movement, the most basic of which is bottom tracking, where the Doppler shift of the last return signal, that of the river bed, is used to determine the motion of the sensor. The assumption here is that the river bed is stationary, so that any Doppler shift in this signal indicates movement of the sensor. As long as the assumption holds that the bed is not mobile, this works well. If the bed consists of fine sediment that moves in the form of bed load transport, the ADCP is no longer able to accurately determine its own movement based on bottom tracking. On the other hand, this feature can also be inversed and used for measuring bed-load movement, using a stationary instrument tracking the movement of the bottom beneath it (Kostaschuk et al., 2005; Ramooz and Rennie, 2010; Rennie and Church, 2010). Claude et al. (2012) used stationary ADCP flow velocity measurements in a series of points along transects in a study of bed-load transport.

The addition of a global satellite navigation system (GNSS) system to the ADCP, preferably a real time kinematic (RTK) system (*cf.* Section 2.3.2), allows the instrument to determine its position and movement accurately without referencing the river bed. This set-up allows ADCPs to be used in moving bed conditions. Rennie and Rainville (2006) and Wagner and Mueller (2011) found the velocity estimates to to be possible within 1 % accuracy using RTK and within about 3 % using SBAS-DGPS (*cf.* Section 2.3.2). Finally, in order to accurately determine the flow directions, a compass needs to be integrated into the instrument, as well as an inclinometer, or better yet, an inertial measurement unit (IMU) that measures the roll, yaw and pitch and velocity and gravitational forces of the instrument and thereby allows compensating any tilting of the instrument while it moves.

Given that the instrument is now able to determine its own position, movement and direction, it can measure a series of flow measurement samples (ensembles) along a transect across a river (Figure 5). In this manner a much denser set of flow measurements can be achieved in a short amount of time than could reasonably be gathered with any other method. Since the ADCP is also able to determine water depth, either using the Doppler beams or, in some cases, a dedicated vertical sonar beam, the cross-sectional profile is also mapped at the same time as the flow

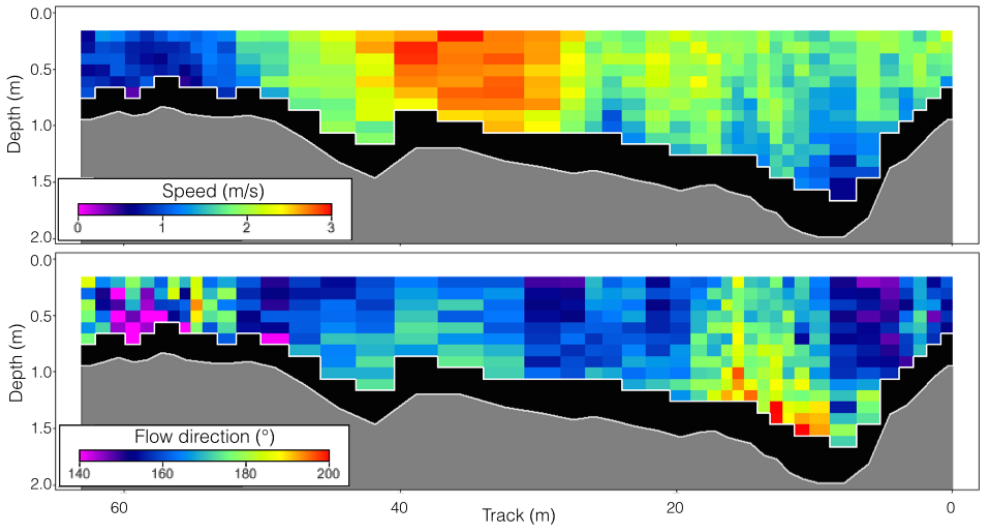

FIGURE 5 Example transects from an ADCP cross-sectional discharge measurement, showing the measurement cells as a raster of flow velocities (top) and directions (bottom), with each raster cell corresponding to one ADCP measurement cell (bin) and each vertical stack of cells being one ensemble, that is one sample. The width of the samples is proportional to boat speed. The black area above the river bed can not be measured reliably due to side-lobe interference of the acoustic signal.

field is measured. Given the detailed flow data combined with an accurate profile, the estimation of discharge using Equation 3 is now a trivial task — in principle. In practice, several aspects need considering though. For one, there is the blanking distance near the sensor that is caused by ringing of the transducer and therefore makes it impossible to measure flow data near the sensor (Muste et al., 2009) (*cf.* Figure 4). Mueller et al. (2007) analysed the accuracy of the flow measurements near the sensor and found that the sensor no longer influences the measurement results at a distance of 0.5 m. In addition to the blanking distance, ADCP measurements suffer from side-lobe interference, which is caused by the angle at which the signal hits the river bed, which causes a stronger reflection to be returned sooner than the signal has fully penetrated the lower layers of the water column, obscuring the weaker return form the water column near the bed. This side lobe interference causes the measurement near the river bed to be impossible, and these data need to be discarded (Nystrom et al., 2007). The thickness of this layer varies with transducer angle and depends on the local bed topography (*cf.* Figure 5). The vertical profiling range affected by side lobe interference ranges between 6 % of depth at at 20° transducer angle to 15 % at a 30° arrangement (Simpson, 2001). Furthermore, discharge computation requires edge estimation, that is, the area near the river bank that is either too shallow for the ADCP to measure, or for the deployment vessel to navigate in, needs to be estimated. Modern ADCPs contain internal algorithms to estimate these values based on a user-input distance value and extrapolation factors.

The vertical beam of an ADCP can be used also for depth mapping. When measuring cross-sections for discharge or flow fields, the cross-sectional profile is integral to the measurement. When applied in an aerial survey pattern, a data set of

point depth measurements can be gathered that yields a bathymetry surface by interpolation (*e.g.* Vericat et al., 2014; Paper IV). Furthermore, it is possible to make use of all the slanted ADCP beams in addition to the vertical beam to in effect simulate a side-scan sonar, by applying geometric corrections to the position of the river bed points based on the slant angle and the position of the sensor (Fitzpatrick, 2012; Manu et al., 2014).

2.2.4 Flow field mapping

Frothingham and Rhoads (2003) mapped 3D flow velocities throughout a meander bend using an ADV on a series of transects in a very thorough and laborious procedure referencing the ADV to a taught steel tag line for each individual transect. More recently Sukhodolov (2012) employed a similar technique for mapping the mean and turbulent flow patterns in a meander bend, again measuring the flow field along transects using an ADV. David et al. (2013) characterised the 3D flow field in a small mountain stream using an ADV.

ADCPs provide a much faster and more efficient way to measure flow fields and they deliver a much denser sample pattern within one transect than an ADV could ever reasonably achieve. Muste et al. (2004b) evaluated the use of mobile ADCP measurements to capture the mean flow field of a river and then compared this to stationary flow measurements (Muste et al., 2004a) finding that the mean flow field can be characterized better when measuring stationary flow at one location over a period of 16 minutes, compared to moving boat measurements that measure a spatially more extensive and continuous series of instantaneous flow measurements. Nystrom et al. (2007) also determined that a four-beam ADCP is necessary to resolve turbulence. While it is certainly true that a time-averaged flow measurement resolves the average flow at one specific location better than a moving boat measurement, there is value in the spatial continuity of the moving boat data.

Most work on flow field mapping, even that using ADCPs, has been conducted using transects (*e.g.* Dinehart and Burau, 2005a; Shields and Rigby, 2005; Nanson, 2010; Petrie et al., 2013; Kasvi et al., 2015) that are either analysed as transects or spatially interpolated to fill in the areas between the measured transects (*e.g.* Jamieson et al., 2011). Kim and Muste (2012) presented a set of tools for extracting additional information from ADCP data and visualising flow data in 2D or 3D transects or a series of transects at the reach scale, including spatial averaging of multiple transects. Parsons et al. (2013) also presented a set of tools specifically designed to process ADCP data to facilitate analysis of transect-based flow fields. Both these tool sets are designed to work with ADCPs developed by Teledyne RDI.

Some work has emerged that tries to characterise the flow field at the reach scale in an areal manner, rather than a linear transect. Lane et al. (1998) mapped the flow field of a small stream using a Total Station to map ADV flow measurements to a coordinate system. More recently, a few researchers have started to use ADCPs in a spatially extensive manner, rather than in linear transects in order to capture areal flow fields and in some cases also bathymetry (Dinehart and Burau, 2005b; Rennie, 2008; Rennie and Church, 2010; Guerrero and Lamberti, 2011; Williams et al., 2013b; Lotsari et al., 2014) making use of RTK-GNSS for precise positioning of the ADCP.

2.3 Bathymetry — surveying the river bed

One of the most challenging environments to measure or model using remote sensing is the underwater realm. At the same time, the submerged part of the river channel is the most crucial part of the channel when it comes to modelling or understanding flow hydrodynamics, sediment transport, fluvial geomorphology or ecology (Merwade, 2009). The combination of the challenge and the demand for the data makes subaqueous remote sensing a very interesting field of research.

The most commonly measured and used parameter of the underwater environment is topography. Other parameters, such as habitat, substrate etc. are in many ways related to topography. Measuring underwater topography usually boils down to measuring water depth and the water surface elevation. Depth can then be subtracted from this elevation in order to obtain the river bed elevation. One notable exception to this principle would be green LiDAR (Kinzel et al., 2013), since that measures the river bed elevation directly [1], without the need for water surface elevation — even though that parameter gets measured as a side effect as well. Another would be the mapping of the river bed by photogrammetry, correcting for surface refraction (Murase et al., 2008). The focus of this thesis in terms of bathymetry lies on optical remote sensing of bathymetry. The term bathymetry refers to the measurement of depth, so that bathymetric model is a model of depths, rather than topography, which refers to terrain elevations, so that underwater topography is a digital terrain model of the river bed in terms of elevation above seal level, rather than depth below the water surface. The following sections give a short background on bathymetric mapping, eventually leading to remote sensing methods and focusing on rivers.

2.3.1 Background on bathymetry

The measurement of depth is known as bathymetry (from Greek: bathy = depth, meter = measure.). Since the early days of shipping, water depth has been of interest and therefore it has been measured. The first systematic studies of bathymetry were conducted at sea in the 1840's using sounding lines, *i.e.* a weighted rope that is lowered from a drifting ship to the sea floor, so that distance can be read off markers on the rope. This method is laborious, slow and limited in precision. An improvement was the Thomson sounding system developed in the 1870's that used a piano wire instead of a rope, improving accuracy by an order of magnitude (Dierssen and Theberge, in press). While mostly used to produce nautical maps, the Australian Navy also mapped 60 miles Hawkesbury River in New South Wales during the 1870's producing about 6500 point measurements spaced about 45 m along transects that were spaced on average at 100 m intervals (Dury, 1967). The nature of this method means that only a limited number of points can be gathered in any reasonable amount of time.

[1] To be perfectly correct, green LiDAR measures the distance of the submerged (or emerged) topography from the scanner and relates that to the scanner's position and inclination.

2.3.2 Positioning

In addition to the depth, the horizontal position of the measurement needs to be determined if any maps of bathymetry are to be created form these measurements. In a river environment this is relatively simpler than at sea, since depths can be measured in a transect that can be relatively precisely located on a map, even without sophisticated positioning equipment, such as satellite positioning. Before accurate satellite positioning became available during the end of the 20th century, elevation differences between measurements were commonly determined using levelling or theodolites (*e.g.* Maxwell and Smith, 2007).

Indeed, the positioning tool itself can be used for mapping underwater topography directly in shallow water, which is very useful in smaller streams where depth and flow velocity allow wading in the river. Total Stations (*e.g.* Fuller et al., 2003; Koljonen et al., 2012; Fuller and Basher, 2013) have been used for mapping river bed topography directly, or for generating depth measurements using RTK-GPS in combination with a water surface interpolation (*e.g.* Paper II; III; Brasington et al., 2000; Westaway et al., 2001; Fuller and Basher, 2013; Williams et al., 2013a).

Global navigation satellite systems (GNSS) encompass the presently operational NAVSTAR global positioning system GPS (USA), and GLONASS (Russia) systems, as well as the GALILEO (EU) and BEIDOU (China) systems that are currently being implemented. Briefly, the positioning of a single receiver is affected mainly by receiver clock error, satellite clock bias, satellite orbital error, ionospheric and atmospheric interference causing delay in the signal, in addition to the multipath signals (*e.g.* Hofmann-Wellenhof et al., 2007). Receiver clock error is the largest error but this can easily be corrected using a minimum of four satellites and determining pseudoranges. All others sources of error listed above, bar multipath signals, are constant within a given geographical area. Differential GNSS is one way to eliminate all but the constant errors by using a base station with an accurately known position. Knowing its position, the base station can determine the error in the pseudoranges to each satellite and the cumulative error this introduces to its position. The base station can then broadcast the necessary corrections to a moving receiver, a rover, either locally or regionally via a radio connection, or, in the case of satellite based augmentation system (SBAS), through a network of geostationary satellites (*e.g.* Hofmann-Wellenhof et al., 2007). This generally results in sub-metre accuracy, compared to tens of metres without corrections. (Some ADCPS, such as the Sontek M9 and S5 use SBAS-DGPS for positioning.) Real time kinematic GNSS positioning, a technique originating in the mid-1990's and commonly used in surveying, is a differential technique that also makes use of a terrestrial base station, but rather than correcting the timing error in the pseudoranges based on the code information carried by the signal from the satellite, it uses the phase of the signal itself. Assuming the base station and the roamer are within close proximity, the influence of the main error sources is the same for both devices, so the phase difference between the base station and the roamer can be used to determine and cancel out these errors. The error in the phase based calculation is much smaller than the code-based pseudo-ranges, but it is affected by phase-ambiguity, which needs resolving. This can be resolved by converging measurements of a single frequency over a long time or using multiple frequencies for a faster solution, giving an accuracy of around 1 cm (*e.g.* Bilker and Kaartinen, 2001; Hofmann-Wellenhof et al., 2007). The RTK- and VRS-GNSS used in all the original

papers of this thesis are based on a dual-frequency RTK solution. The virtual reference station (VRS) system, also known as network-RTK is a newer development of the RTK principle, using a network of connected permanent base stations to compute the corrections for a rover anywhere within the network, and transmitting this correction via a mobile Internet connection. Paper IV explains this system in more detail. A more detailed discussion of the different GNSS positioning systems and dilution of precision involved in the measurements is beyond the scope of this work.

The horizontal accuracy of RTK-GNSS systems is typically better than 0.02 m with the vertical generally about 1.5 times the horizontal accuracy expressed as RMS error (Bilker and Kaartinen, 2001). Fuller and Hutchinson (2007) limited set the acceptable vertical accuracy limit of RTK-GPS points at 0.05 m — as was done in Paper IV — but they found actual accuracies to be around 0.02 m. Vertical positioning is most challenging in moving measurement applications such as mobile mapping systems (MMS) or moving boat ADCP flow measurements. The high sampling frequency required by these applications pushes the limits of what GNSS can deliver, even in RTK mode. Any irregularity that can occur in the high-frequency GNSS elevation measurements, particularly in the vertical dimension, can be corrected by combining the GNSS position data with IMU data.

2.3.3 Sonar

The invention of sonar in 1913 brought about a great advance in depth mapping. The system is akin to radar (hence the name, SOund Navigation And Ranging), also known as echo sounding. A transmitter emits a sound wave that bounces off an object in the distance, i.e. the sea floor or river bed, but possibly also other objects, such as fish or boats. The signal then travels back from the object towards a receiver, usually mounted at the same location as the transmitter, that then records the travel time of the signal. This measured travel time is converted to range by multiplying half the travel time in seconds by the speed of sound in metres per second. Assuming the transmitter and receiver are positioned so that the signal propagation is vertical, range equals depth; otherwise, depth needs to be calculated by correcting for the angle of inclination (*e.g.* Kolev, 2011).

The speed of sound in water is not constant and needs to be determined accurately for the location and conditions, if return times are to be correctly converted to ranges. The speed of sound is affected primarily by the temperature, salinity and pressure, i.e. the density of the local water column. The speed of sound in water averages 1500 ms^{-1} and increases with increasing temperature, increasing salinity and increasing pressure, i.e. increasing depth. In river settings, temperature is the only variable that really affects the speed of sounds since rivers generally carry fresh water and they are mostly sufficiently shallow for the pressure increase with depth to be negligible. Temperature may need to to be taken into account though, as do abrupt changes in temperature through thermoclines. In such conditions a sound velocity probe needs to be employed in order to get accurate measurements. Nowadays a conductivity, temperature and depth probe (CTD) that gives information on all three variables affecting sound propagation is generally used in hydrography (*e.g.* Möller et al., 1995; Patterson et al., 2011; Gelfenbaum et al., 2013) and also to correct the speed of sound in ADCPs.

Sonar has been widely used to map river bathymetry along transects (*e.g.* Dury, 1970; Kiss and Sipos, 2007; Maxwell and Smith, 2007) that can be interpolated for instance into a triangulated irregular network (TIN) (Milne and Sear, 1997; Hardy, 1998). Schäppi et al. (2010) developed an interpolation method specifically intended to interpolate river transects into a continuous surface, or it can be used from a moving boat to cover a larger area (*e.g.* Rogala, 1999; White and Hodges, 2005; Merwade, 2009). These data can be interpolated to create a model of the underwater topography. Merwade (2009) analysed the effect of interpolation method used on the river bed model results. While the accuracy of the depth at the location of the points measured with a single-beam sonar is very good (up to 1 cm, depending on the equipment used), the quality of the result of the interpolation depends largely on the density with which the points were collected and benefits from a systematic and closely spaced sampling method (Rogala, 1999; Merwade, 2009).

Swathe-sonar, that is either multi-beam sonar used to map bathymetry based on ranging, or side-scan sonar used for imaging of the submerged topography based on signal intensity, are used to cover larger areas than single-beam sonar can. Multi-beam sonar is frequently used for mapping bathymetry in marine environments (*e.g.* De Moustier and Matsumoto, 1993; Kostylev et al., 2001), as it allows to map the bathymetry of a relatively wide area at once based on ranging. The with of the beam, however, is positively correlated to water depth. This hinders swathe sonar usage in fluvial environments compared to oceans since rivers are often shallow, which means that this system could only cover a small area of river bed at any one time. Nevertheless, multi-beam sonar (Parsons et al., 2005; Claude et al., 2012) and side-scan sonar (Sirniö, 2004; Maxwell and Smith, 2007; Manley and Singer, 2008; Kaeser et al., 2013) can provide wider coverage than single-beam sonar also in rivers .

In this study (Papers I, II, III), sonar has been used primarily for gathering single-point reference data for calibrating remote-sensing based models. In Paper IV vertical beam data from the ADCP, which are basically sonar points, were interpolated to create a series of bathymetric models.

2.3.4 Remote sensing of bathymetry

The use of remotely sensed data for mapping bathymetry was pioneered in oceanography, particularly in coastal zone research (Lyzenga, 1981; Gould and Arnone, 1997; Kohler and Philpot, 1998; Sandidge and Holyer, 1998; Lee et al., 1999; Roberts and Anderson, 1999). The focus here is on passive optical imagery, which records reflected sunlight, as opposed to LiDAR, which records the return signal of an actively emitted frequency. Due to the way that solar radiation gets absorbed rapidly by water, the maximum depth that visible light can penetrate is limited (Lillesand et al., 2008), hence the applicability of remotely sensed data for depth measurements is limited to shallow water areas. The mapping of water depth from images requires clear water and an unobstructed view of the river bed in the area to be mapped.

The earliest efforts of remotely sensing water depth in coastal areas date back to World War II where Lundahl (1948) used photogrammetric techniques as well as aerial photography based methods to derive depth from changes in wavelength as ocean waves enter shallow waters. While direct determination of water depth by photogrammetry has been explored (*e.g.* Fryer and Kniest, 1985; Murase et al., 2008), it is beyond the scope of this work.

During later years, most research relevant to optical bathymetric mapping focused on understanding the optical characteristics of water (*e.g.* Lyzenga, 1981; Gould and Arnone, 1997; Holden and LeDrew, 2002; Lyzenga et al., 2006; Sagawa et al., 2007). This research helped to establish the physical basis for the techniques used in remotely sensed bathymetry mapping in rivers as well.

In near-shore oceanic environments the use of satellite imagery was found to be useful (Liceaga-Correa and Euan-Avila, 2002; Lafon et al., 2002; Stumpf et al., 2003; Doxani et al., 2012), despite its much coarser spatial resolution, as the areas under consideration here are large and do not suffer from the kind of problems that plague analysts of rivers, such as overhanging trees, shadows and turbidity. Furthermore, some of the techniques, such as the widely used Lyzenga algorithm (Lyzenga, 1981), require parameters that can only be truly measured in deep water environments. While the empirical determination of the deep water reflectance is a simple matter in oceanic environments where depths often go well beyond the maximum penetration of light not far off the shore, it is often impossible to find an area where bottom reflectance has no influence in a much shallower fluvial setting Paper II.

Research on remote sensing of rivers focuses on river morphology (Wright et al., 2000; Gilvear et al., 2004) and in stream habitat mapping (Marcus, 2002; Anandakumar et al., 2008) as well as bathymetry modelling. Several studies have dealt with a combination of these aspects (*e.g.* Legleiter et al., 2004) while others (*e.g.* Liu et al., 2003; Koponen, 2006) have used remotely sensed data to monitor other water quality parameters such as suspended sediment or phytoplankton load in rivers and lakes or aquatic vegetation in lakes.

A variety of sensors are available for fluvial research, ranging from panchromatic and colour photo– and videography to multispectral and hyperspectral scanners (Bryant and Gilvear, 1999; Gilvear and Bryant, 2005; Carbonneau and Piégay, 2012). Generally airborne imagery is found to be more useful than satellite data for river monitoring, due to its higher resolution and potentially flexible timing, which allows for easy comparison with more traditional field data (Roberts and Anderson, 1999). Lyon et al. (1992) initiated the use of remotely sensed data to compute river bathymetry and bottom sediment types using a radiative transfer model. Winterbottom and Gilvear (1997) used multispectral aerial photographs to map the bed morphology of a gravel bed river in Scotland using both panchromatic and multispectral images. In their study, which was the first to concentrate exclusively on remotely sensed depth modelling, they achieved good classification results in shallow water areas, but the relationship between modelled and measured depths deteriorated slightly in the deeper sections. A later study (Gilvear et al., 2007) also came to the conclusion that while optically remotely sensed depth mapping is indeed possible, it is somewhat limited to shallow waters.

Wright et al. (2000) used multispectral digital imagery together with field data to classify hydromorphologic stream units while Marcus (2002) achieved higher accuracy in mapping in-stream habitats using 1 m resolution 128 band hyperspectral imagery than with ground-based surveys. In a related study Marcus et al. (2003) used the same data to calculate stream depths as well and found that accuracy decreased in smaller streams. Westaway et al. (2003) have applied the use of photogrammetry to produce a DEM of a stretch of braided river valley in New Zealand and used image analysis to compute river depth estimates using Lyzenga's (1981) model, thus completing the DEM by including wet-bed elevation to create a contiguous surface.

Legleiter et al. (2004) evaluated several models for mapping river morphology and in-stream habitats and concluded that the physical basis for remote sensing of rivers is sound, providing a solid foundation for large-scale, long-term mapping and monitoring of fluvial systems. Jordan and Fonstad (2005) used aerial photography to calculate stream power, which involved deriving cross-sectional depth information from the remotely sensed data. Legleiter and Roberts (2005) used a radiative transfer model coupled to a range of simulated scenarios of river morphology and substrates in order to evaluate depth retrieval. They found that while the upwelling spectral radiance can be highly sensitive to river bed shape and material, the use of a band ratio is robustly related to depth, even considering fine scale bottom morphology and patchy substrates. The relationship between the spatial resolution of the sensor and the channel morphology was found to be of major importance, as well as the realisation that the accuracy of image-derived depth estimates are spatially variable over the monitored area. Javernick et al. (2014) used UAV-based photography with a ratio-based log-transform model to map shallow water bathymetry. Ratio-based models rely on the differential attenuation of different frequencies of the visible spectrum in the water column (Figure 6b). Longer wavelengths are absorbed faster and shorter wavelengths penetrate further. This is why in shallow water, using RGB images, the red and green bands are often found to be more useful than the blue band (*e.g.* Winterbottom and Gilvear, 1997; Legleiter et al., 2004; Carbonneau et al., 2006; I), because blue does not vary with depth until deeper water is reached. Fonstad and Marcus (2005) developed a novel approach to modelling river depth from remotely sensed data, based on image brightness values coupled with theoretical hydraulic equations. Their hydraulically assisted bathymetry (HAB) model combines local discharge information, channel width and slope along with discharge and velocity equations to compute cross-sectional depth estimates, which are subsequently used to compute the depth value for each pixel in the remotely sensed image. Their aim was to create a model that is not based on empirical depth values but only requires discharge to be measured on the ground. All other data can be derived from remotely sensed data or maps, which could widen the field of its practical applicability. The authors were able to achieve moderately accurate representations of two test rivers using virtually no ground data. This method is explained in more detail and evaluated for accuracy in Paper I. Walther et al. (2011) also evaluated the HAB 2 model, concluding it to be useful with some constraints. Carbonneau et al. (2006) focused on depth calibration problems occurring with aerial photography based data collection stemming from differences in light conditions during the period of data acquisition over a large area such as a whole river or catchment area. Their findings showed a substantial increase in depth model quality when first applying their illumination correction, which is based on the identification of areas with near-zero water depth in different images. While the precision level of 15 cm in depth is lower than can be achieved with ground measurements, they argue that the increased horizontal coverage more than makes up for that relative deficiency, a view shared by many of their colleagues (*e.g.* Marcus and Fonstad, 2008).

Modelling bathymetry from optical imagery relies on the observation that the deeper areas of water look darker than the shallow areas. This is a manifestation of Beer-Lambert's law of logarithmic decay, that in the case of a water body with minimal refraction, explains the exponential absorption of light as it penetrates the

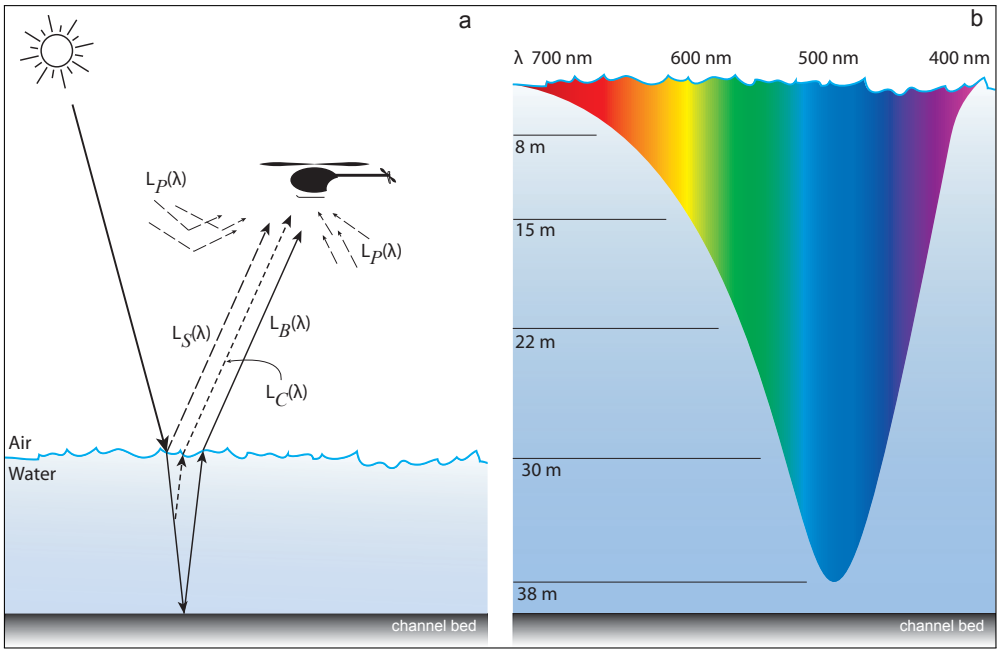

FIGURE 6 (a) Diagram of the components involved in the radiative transfer leading to the at-sensor radiance signal: $L_C(\lambda)$ is reflectance in the water column, $L_S(\lambda)$ is reflectance off the water surface. Adapted from Carbonneau and Piégay (2012) and Bukata et al. (1995). (b) Illustration of the attenuation of different wavelengths of the visible and near-visible spectrum in clear water. Adapted from Morris (2009).

water column:

$$I = I_0 e^{-\beta D} \tag{6}$$

where e is the base of natural logs, I is the intensity of light at a given depth, I_0 is the intensity of light immediately prior to entering the water column, β is the attenuation coefficient and D is the distance that the light passes through water. In optically shallow water where the bottom is visible, D equals depth. Attenuation is the result of both absorption and scattering of light as it travels through the water column (Herlevi, 2002).

The full radiative transfer of solar irradiation to an optical sensor (Figure 6a) involves diffusion and scattering of the incoming solar irradiation in the atmosphere ($L_P(\lambda)$), partial reflectance off the water surface ($L_S(\lambda)$), absorption, diffusion and reflectance in the water column ($L_C(\lambda)$), reflectance off the stream bed ($L_B(\lambda)$). The composition of the upwelling spectral radiance ($L_T(\lambda)$) measured at an imaging sensor above a river channel for a given wavelength (λ) thus consists of (Legleiter et al., 2009):

$$L_T(\lambda) = L_B(\lambda) + L_C(\lambda) + L_S(\lambda) + L_P(\lambda) \tag{7}$$

The Beer-Lambert law is the cornerstone of physics based bathymetry models that aim at modelling depth by accounting for the radiative transfer governing the light eventually recorded in the remotely sensed image (Legleiter et al., 2004). The HAB 2 model (Fonstad and Marcus, 2005) used in Paper I for instance, estimates the

rate of absorption of light in the water column to calculate depth. The general aim of physical models is to establish a generally applicable model of the light-atmosphere-water column-imaging sensor chain in order to be able to apply them more generally than in a specifically calibrated area based on ground depth measurements. While physics based models find more acceptance in the mapping of coastal environments in which remote sensing has a longer history, empirical models are favoured in river environments thus far (Legleiter and Fonstad, 2012).

Empirically based models, such as the widely used Lyzenga (1981) model (Papers I, II and III) estimate depths based on a regression of field-measured depths and radiance values measured in a remotely sensed image. Aside from delivering good results within the area of calibration, these models also implicitly account for atmospheric influences that are part of the radiative transfer, which eliminates the need to quantify them, as in physical models. The requirement of empirical ground data takes away one of the major advantages of remote sensing technology, which in principle aims at retrieving information remotely, without the need for ground data. On the other hand, even such endeavours require ground truthing if the accuracy of the information is to be quantified, so that requirement only represents a minor disadvantage.

Charlton et al. (2003) evaluated aerial LiDAR (ALS) (*cf.* Section 2.4.2) for mapping river environments and obtained mean errors of better than 0.2 m on exposed gravel areas, but the performance in the submerged areas deteriorated to about 0.7 m vertical error, with the deeper areas not giving any returns. Like aerial photography based methods, LiDAR is also limited by turbidity, although to a somewhat lesser extent, due to the active signal used. Unlike the infrared LiDAR generally used for topographic surveying, green LiDAR (*e.g.* Tetis, 2010; Kinzel et al., 2013) is able to penetrate the water column (*cf.* Figure 6b). Green LiDAR is therefore also referred to as bathymetric LiDAR. Aerial bathymetric LiDAR in fact uses both a red and a green laser, with the red beam detecting the water surface and the green beam detecting the river- or, more often, the sea bed. The footprint of the green laser beam on the submerged ground surface is rather large, increasing with depth up to several metres in diameter, due to the refraction of the light at the water surface. This limits the vertical accuracy just by virtue — or vice, rather — of being unable to determine a precise reference point on a naturally shaped surface if the area captured by one laser point is several m^2 in size (Tetis, 2010). The large footprint also limits the use of aerial bathymetric LiDAR to larger rivers. Smith et al. (2012) used a TLS system with a green laser to map shallow water bathymetry at very high resolution by applying a correction for the refraction of the laser beam as it penetrates the water surface at an angle. Recent developments in multispectral LiDAR (Hakala et al., 2012) may also prove useful for bathymetric mapping in the future.

2.4 Topography — surveying the flood plain

Surveying the topography of the floodplain of a river channel can be conducted using a GPS or tacheometry.

Tacheometry is the measurement of the location of one point relative to another known point using, at its most basic, a level and a tape measure. The Total Station is the modern fully automatic version of this survey technique that automatically measures distance and angles of a survey pole relative to the station itself, with millimetre accuracy. A further discussion of this measurement technology is beyond the scope of this work since it was not used in any of the studies presented here.

These techniques, while very precise, are designed primarily to measure single reference points, rather than to conduct a systematic survey of the topography of a large area. Nevertheless, given enough time, they can be used to this end too. Brasington et al. (2000) surveyed a 200 by 80 m reach in a very dense pattern of RTK-GPS and tacheometry point measurements, yielding almost 1 point m^{-2}. Wheaton et al. (2010) used repeated total station surveys to conduct change analysis for investigating the effect of river restoration projects on ecohydraulics. Fuller and Hutchinson (2007) surveyed at a variable point density according to scale and topographic features with an average point density of 0.1 point m^{-2}. Lotsari et al. (2013) surveyed exposed point bars in a 5 km by 900 m braided reach using RTK-GPS. This level of topographic survey benefits tremendously from remote sensing techniques that allow to capture the topography of relatively large areas in a short amount of time at a density that would be hard to achieve using direct measurements. Remote sensing of topography can be divided into photogrammetry and laser scanning.

2.4.1 Photogrammetry

Photogrammetry describes the process of capturing quantitative information from images. In a geographical context, this generally means the measurement of landforms or terrain from either aerial or terrestrial photography. Photogrammetry relies on the stereo geometry of one point in the landscape that is represented in at least two different photographs with a slightly different angle of view. A detailed discussion of the principles of photogrammetry is beyond the scope of this work. A brief outline of the principle involved is followed by an overview of the use of photogrammetry in river research. Traditionally, photogrammetry relied on the stereo geometry of two cameras and their internal geometry of the lens and the film, or more recently the digital sensor, to be known quantities, so that other parameters, such as distance to the target could be calculated. This traditionally requires analog plotters that reproduce a scaled down version of the original geometry used to capture stereo images. This is very limiting in the equipment that can be used and costly to operate(Lane et al., 1993). Analytical methods developed in the 1980's allowed the calculation of both the position of a point on the ground based on the known camera position and orientation and system geometry, but conversely, also allowed to position the sensor based on a set of known points on the ground (Chandler and Moore, 1989). In addition to aerial stereo photography, analytical photogrammetry can also be applied to oblique terrestrial images. Lane et al. (1993) investigated the use of photogrammetry in geomorphological investigations, highlighting the benefits of analytical photogrammetry vs. the older, mechanical approach. Later, digital oblique photogrammetry was used for monitoring monitoring river-channel change at high temporal resolution (*e.g.* Pyle et al., 1997; Chandler et al., 1998, 2002). Photogrammetry can produce both topographic measurements in the form of digital terrain models (DTM) and orthorectified photographs, or orthophotos, that is, aerial

photographs that are processed to have the geometry of a map. In the last decade, structure-from-motion photogrammetry has emerged as an alternative that is simpler to implement and relies on software to solve the geometry of randomly placed images that cover the same target area. This has only become feasible since the necessary computing power has become available. Structure-from-motion does not require a stereo camera set-up, but relies on finding the same point in different images through pattern recognition algorithms (Carbonneau et al., 2010) and then solves the camera's position at the time of taking the image relative to these points, producing a 3D point for each recognised target. This results in a point cloud similar to the ones produced by terrestrial LiDAR, but typically less dense. A small amount of ground control points is required to georeference the point cloud. These control points also serve as a starting point for the pattern finding algorithms.

Fonstad et al. (2013) recently investigated the use of structure-from-motion photogrammetry for fluvial research and found the results to be on par with aerial LiDAR in density and at centimetre accuracy. In Paper III structure-from motion UAV-photogrammetry is evaluated against TLS for mapping floodplain and riparian topography and in Papers II and III the orthophoto generated in the process is used as input for the high-resolution optical bathymetric models. Others (*e.g.* Javernick et al., 2014; Tamminga et al., 2014; Vericat et al., 2014) have more recently also used aerial photogrammetry in combination with other technologies to map river topography. The increase in computing power in recent years has has led to great advances in analytical photogrammetry, reducing the physical requirements of the camera systems used to the point that recent investigations (Micheletti et al., 2014) are looking into the potential of smartphone photography using structure-from-motion photogrammetry for mapping river channel changes. Lane et al. (1993) discussed the clear advantage of photogrammetry over field-based measurements of landforms in that the whole terrain is captured and can be analysed later, as opposed to the surveyor having to decide in situ what parts are important and need to be measured, due to his inability to capture the whole picture. That is an important point that relates not only to photogrammetry, but remote sensing in general, and in particular also to laser scanning, described below.

2.4.2 Laser Scanning

Since the beginning of the current century, laser scanning, also known as LiDAR, has become increasingly commonly used for topographic mapping in river research (*e.g.* Mertes, 2002; Bates et al., 2003; Milan et al., 2007; Alho et al., 2009a; Entwistle and Fuller, 2009; Heritage and Milan, 2009; Alho et al., 2011b; Vaaja et al., 2011a; Williams et al., 2011; Bailly et al., 2012; Kasvi et al., 2012; Saarinen et al., 2013; Vaaja et al., 2013). An extensive review of laser scanning applications in river research can be found in Hohenthal et al. (2011).

Laser scanning makes use of an actively emitted laser light, that is a beam of coherent light, *i.e.* light waves of the same frequency and wavelength, to measure the distance between the sensor and a remote object. The measurement can be based on ranging of a series of short laser pulses, where distance is measured as half the return time of the laser pulse times the speed of light. Instead of pulsing laser, a continuous beam can be used in which case the range is determined based on the phase difference of the emitted beam of a specific wavelength and the received return signal. Full

waveform laser scanners are able to resolve not only the main return signal, but a host of intermediate weaker returns caused by objects that are located in between the scanner and the main reflecting object, often the ground (Wagner et al., 2004). Laser scanners produce a point cloud of location points relative to the scanner based on the range and angle of the laser beam measured. In order for these point clouds to be oriented in a geographical coordinate system it is necessary to either know the precise location and orientation of the scanner at any moment during the scan, or for there to be known reference targets often in the form of round spheres, located inside the area to be scanned, or both.

Laser scanners can be deployed on an aircraft, *i.e.* aerial laser scanning (ALS), in order to map large areas. This generally results in a relatively large laser footprint, that is the size of the laser beam as it impacts its target, often in the order of 0.5 to 2 m, depending on the flying height. This is adequate for producing DTMs of large areas rapidly. Although ALS can be useful in some hydromorphological investigations (*e.g.* Cobby et al., 2001; Mandlburger and Brockmann, 2001), the vertical view and large footprint can cause large parts the river banks not to be adequately captured (Alho et al., 2009a). Most river researchers have found terrestrial laser scanning (TLS) more useful. TLS generally refers to a tripod-mounted fixed position laser scanner, whereas mobile laser scanning (MLS), which is also terrestrial, refers to scanners mounted on moving platforms, such as cars (Jaakkola et al., 2010), boats (Alho et al., 2009a), or portable systems (Kukko et al., 2012). Tripod mounted laser scanners achieve the highest accuracy of any of these systems.

Dufour et al. (2013) evaluated aerial laser scanning (ALS), satellite radar and UAV-photography for mapping and monitoring riparian vegetation. Saarinen et al. (2013) modelled riparian vegetation using the ROAMER mobile mapping system — an updated an lighter version of the AKhKA system used in Paper III— to gather mobile laser scanning data in combination with UAV-photography.

2.5 Merging topography, bathymetry and flow

Hydromorphology, whether for research or management, needs information of the whole river system, so it makes sense to merge the different methods outlined above in order to get a synoptic view on rivers, attempting to meet the potential outlined by Gilvear et al. (2004). Lane et al. (1994) used analytical photogrammetry and later (Chandler et al., 2002) used oblique photogrammetry to model flood plain topography and combined this with an interpolated submerged channel based on Total Station point measurements for change detection purposes. Moretto et al. (2013) and Delai et al. (2014) create hybrid topography using LiDAR and optical bathymetry, both using a model by Moretto et al. (2012) the details of which are not published. Williams et al. (2013a) merged terrestrial LiDAR and Javernick et al. (2014) aerial photogrammetry with optical bathymetric methods for mapping seamless riverine topography. Vericat et al. (2014) are working in a similar direction of the present work, integrating UAV-photogrammetry based point cloud topography with ADCP-based bathymetry. Recently Tamminga et al. (2014) used UAV-based photography with a ratio-based log-transform model to map shallow water bathymetry and photogrammetry

to model the dry part of the flood plain from the same image set. These recent publications using UAV-based photography and structure-from-motion photogrammetric techniques or LiDAR, similar to Paper III indicate that this is one promising means of mapping continuous, seamless river topography. In the same vein, the recent work on spatially continuous ADCP surveys for flow field mapping (Williams et al., 2013b; Guerrero and Lamberti, 2011) and interpolation methods for 3D flow data (Tsubaki et al., 2012) indicates the direction in which progress is being made in this field. The methodology presented in Paper IV contributes to this progress.

This thesis combines these two, as yet still separate fields of river remote sensing and presents a new, unified river model consisting of the seamless wet-dry topography of the active river channel and the flood plain including the riparian environment, complemented by the 3D model of 3D flow vectors. This unified model pours the water into the riverine landscape.

3 STUDY AREA

The work presented in this thesis focuses on Northern Lapland. Even though the methods used and developed here are applicable in rivers elsewhere, the geographical context here is focused on the sub-Arctic. This is a challenging environment, in particular for passive optical remote sensing, due to the insolation angle at high latitudes.

This research is also part of a larger research effort by the Fluvial Research Group of the Department of Geography and Geology of the University of Turku focused on this area (Alho et al., 2009b; Kasvi et al., 2012, 2013, 2015; Lotsari et al., 2010, 2013, 2014; Vaaja et al., 2013; Saarinen et al., 2013; Wang et al., 2013).

The study areas are all located in the Tana river watershed. The study sites in Papers I and II are located on the Tana river itself. Papers II, III, and IV are located on one of the Tana's tributaries, the River Pulmankijoki.

3.1 Tana river

The Tana river basin (Tenojoki in Finnish, Tanaelva in Norwegian) is located in the northernmost part of Fennoscandia. The catchment area is approximately 16000 km^2 in size, of which 68 % is located in Finnmark in Norway and 32 % in the province of Lapland in Finland (Mansikkaniemi, 1972). It belongs to the sub-Arctic zone of Fennoscandia and drains an extensive upland area of fell country into the Barents Sea.

The River Tana is 330 km long, unregulated, and forms the border between Finland and Norway for much of its course. The average discharge of the river over the year measured at Polmak is 168 m^3s^{-1} with the lowest discharge in March (41 m^3s^{-1}), the highest discharge in June (544 m^3s^{-1}) and a yearly average high discharge of 1600 m^3s^{-1} (Alaraudanjoki et al., 2001).

FIGURE 7 Map and orthophotos of the study areas. AOI 1 is in Garnjarga on the Tana River (Paper I), AOI 2 is just upstream of Tana Bru, also on the Tana River (Paper II), AOI 3 is the Pulmanki River upstream of Lake Pulmanki (Papers II, III and IV). The Tana River watershed is indicated in grey in the small scale map insert.

3.1.1 Garnjarga

Study area AOI 1 (Paper I) is located at Granjarga between 27°6′24″ and 27°9′47″ E and 69°55′10′ and 69°56′6″ N (Figure 7). The area of interest (AOI) is 2.7 km long starting 3 km downstream of the confluence of the river Utsjoki. This area is located on a relatively short stretch of river where accurate discharge data is available together with excellent quality aerial imagery. The channel in this section consists of large gravel and rather stable, compared to the sandy river bed further downstream. Furthermore, the section contains a range of depths, and reasonable ground data for bathymetry modelling are available as well.

3.1.2 Tana Bru

One test site (AOI 2) in Paper II is located near Tana Bru. This area was chosen because it contains a pool deep enough to retrieve deep water radiance so that the estimation algorithm presented in Paper II could be tested against observed values. The riverbed substrate at this site consists mostly of large gravel in deep areas with strong current, similar to Garnjarga, and some sand in the shallows where the current is weaker.

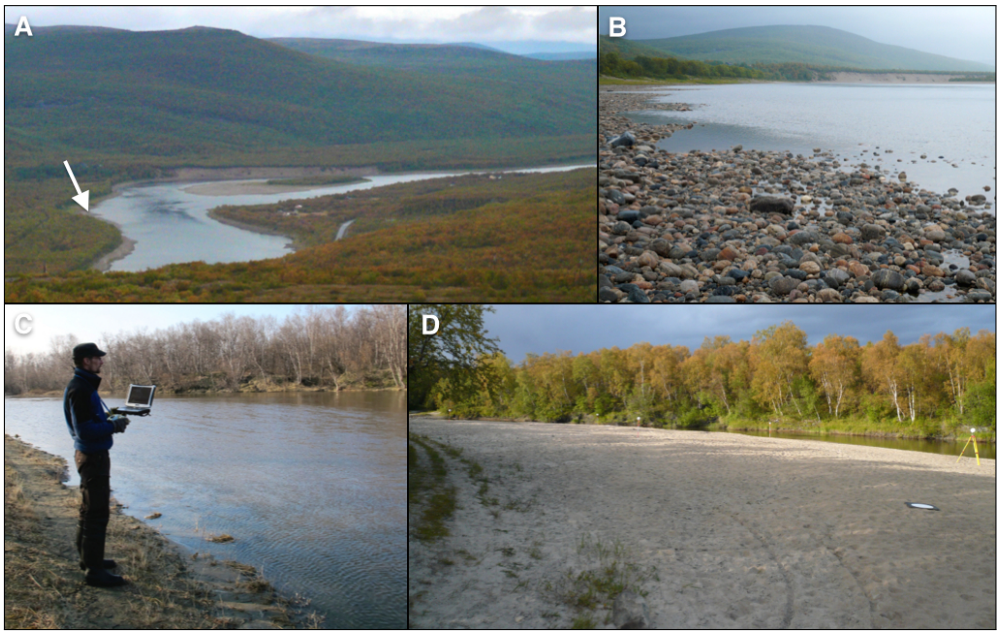

FIGURE 8 (A) The Tana river at Garnjarga (AOI 1) photographed from Ailigaistunturi in Utsjoki, looking downstream. The arrow indicates the position photograph B was taken from. (B) Garjarga on the Norwegian shore looking downstream, giving an indication of the gravel that makes up the river bed in that area. (C) The "Venesärkkä" meander bend in Pulmanki (AOI 3) during the spring flood data collection. (D) The same area from the same point of view as in C during summer low flow showing the exposed point bar. A ground reference target for the UAV imagery can be seen on the sand and a ball-type target for laser scanning is mounted on a tripod near the water's edge.

3.2 Pulmanki river

The second test area in Paper II and the main site for Papers III and IV is a meander bend of the river Pulmanki (AOI3), located (69° 56′ N, 28° 2′ E). The River Pulmankijoki flows northwards into Lake Pulmanki, and continues on the Norwegian side as the River Polmak, to merge with the River Tana at Polmak. The Pulmankijoki flows in a valley of glaciofluvial deposits from the last glaciation, surrounded by fells. The river is about 20–30 m wide during summer low flow, depending on the water level, and the riverbed consists of sandy sediments. Kasvi et al. (2012) and Alho and Mäkinen (2010) describe the geomorphology of this study site in great detail. The typical discharges of the river Pulmanki vary between about 4 m^3s^{-1} during summer low flow and about 60 m^3s^{-1} during the annual snow-melt induced spring flood. The water level can be two to four metres higher during flood time than during summer low flow, depending on the size of the flood. This flow regime combined with the unstable sediments make this a very dynamic river (Mansikkaniemi and Mäki, 1990) that is ideal for change detection studies.

4 MATERIALS AND METHODS

4.1 Data collection

4.1.1 Remote controlled vehicles

The high resolution data used at the reach scale as part of the unified river modelling methodology used in this work is based on remotely controlled vehicles. The data acquisition methods and processing methods used in the papers of this thesis are outlined in Table 1. There are two basic ways in which high resolution can be achieved: either by increasing the sensor resolution, such as a larger amount of pixels in a camera sensor, possibly in combination with a larger sensor, or by reducing the distance between the sensor and the object to be measured, resulting in a larger amount of data points measured, without increasing the sensor resolution. That is, a shorter distance to the subject increases the number of data points per unit area and decreases the measured size on the ground for those data points, be they image pixels, laser points or ADCP flow cells/bins.

4.1.1.1 Unmanned aerial vehicle (UAV)

One way to achieve short distances between sensor and target for aerial imaging is to deploy the sensor, that is, the camera, on a remotely controlled helicopter or airplane, also known as an unmanned aerial vehicle (UAV), or unmanned aerial system (UAS). Some (Smith et al., 2009) have deployed cameras on kites as an inexpensive method of getting a sensor airborne at close range. The term UAS emphasises the combination of aircraft and sensor, possibly combined with on-board GNSS-positioning and IMU, whereas the term UAV refers more generically to an unmanned aircraft. Since unmanned aircraft are commonly used for collecting data, they generally include some sort of sensor and UAV is commonly used in that meaning, more or less synonymously with UAS. Some UAVs used for entertainment purposes do not include any sensors, but even toy helicopters nowadays often carry cameras.

TABLE 1 Data and data acquisition methods and processing methods used in the papers of this thesis.

Paper	I	II	III	IV
Aerial photography (high altitude, medium resolution)	X	X		
UAV-aerial photography (low altitude, high resolution)		X	X	
Orthophoto mosaics		X	X	
Photogrammetry point clouds			X	
Lyzenga optical bathymetric model	X	X	X	
HAB optical bathymetric models	X			
Deep water correction estimator		X	X	
ADCP bathymetric model				X
Depth model (bathymetry)	X	X		
Underwater DTM (bathymetry)			X	X
TLS DTM			X	
MLS DTM			X	
Seamless DoD (TLS + MLS + optical bathymetry)			X	
RTK-GPS	X	X	X	
VRS-GNSS			X	X
Sonar	X	X		
ADCP depth soundings		X	X	X
ADCP flow field				X

Other than the close range they can achieve, UAVs offer great flexibility in gathering data, both spatially and temporally. UAVs can be transported even to fairly remote locations and be deployed rapidly, and — once purchased — at low cost. Preparations on site take less than an hour. In case ground reference targets are needed for georectification of aerial images for instance, their set-up can take much more time than it takes to get the UAV airborne.

Regulations differ greatly from one jurisdiction to another, with some places requiring lengthy permit applications and others allowing great freedom. Generally though, UAVs are to be flown within line-of-sight of the pilot and maximum distances and flying heights are often specified in local regulations (Zinke and Flener, 2013).

Papers II and III make use of UAV photography both for creating orthophotos that are used to create bathymetric models, and in Paper III also for generating a photogrammetry-based 3D point cloud of the channel topography. In 2010, a regular 800-class Minicopter Maxi-Joker 3DD radio controlled single-rotor helicopter was used (Figure 9) with a 12.3 megapixel Nikon D5000 camera with a 14 mm F/2.8 Samyang lens with a diagonal viewing angle of 94°. In 2011 a 700-class Align T-Rex 700E single-rotor RC helicopter was used embarking a 16.2 megapixel Nikon D5100 with a 20/2.8 AF-D with a diagonal viewing angle of 71°.

The payload capability of different UAV models vary widely and also affect flight duration, which typically varies between 5 and 15 minutes (Jaakkola et al., 2010). Heavier loads drain the batteries quicker, so flight time needs to be reduced compared to lighter loads.

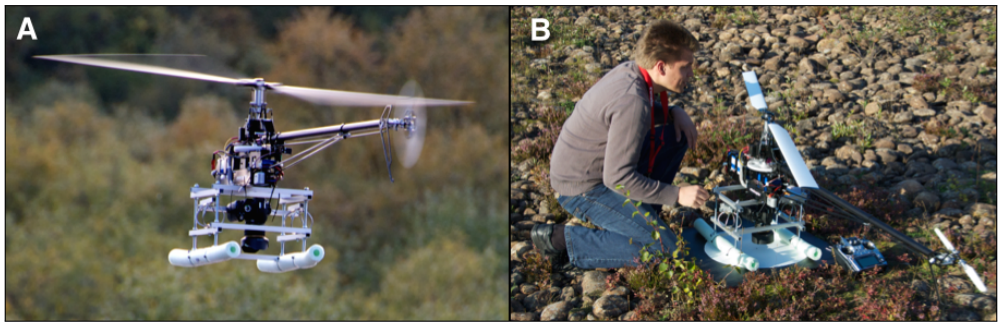

FIGURE 9 A. Minicopter Maxi-Joker 3DD UAV with a Nikon D5000 onboard; B. UAV sitting on a ground control reference target before take-off. Pilot for scale.

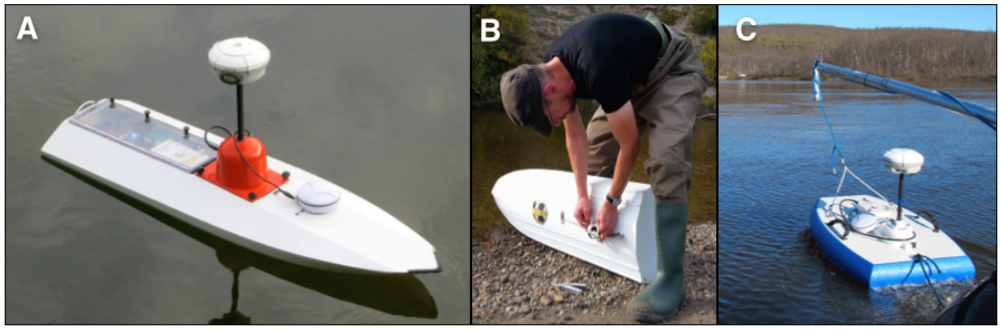

FIGURE 10 ADCP deployment methods: A. RCflow custom-built remote controlled boat with a Sontek M9 ADCP with a Trimble R8 GNSS receiver in addition to the M9's DGPS antenna; B. RCflow from underneath, showing the ADCP transducers emerging from the hull. Operator for scale; C. Sontek S5 ADCP deployed on a tethered Hydroboard.

4.1.1.2 Remote Controlled Boat (RCB)

In the same way that a UAV allows a greater level of flexibility compared to a manned aircraft, a remote controlled boat allows more flexibility compared to a full-sized boat. In this thesis (Paper IV), a custom-built remote controlled boat, RCflow , was used to conduct ADCP measurements. The boat was designed to fit a Sontek M9 ADCP sensor and control unit, along with a second GNSS antenna (Figure 10a). The sensor fits flush to the hull that was designed to minimise drag and turbulence that would interfere with the acoustic measurement (Figure 10b). Muste et al. (2009) demonstrated turbulence cause by the immersed sensor and its deployment platform can cause the uppermost measurement cells to be invalid and the hull design tries minimise this effect.

The remote controlled boat has several major advantages over a manned boat: it can access very shallow water, it is easy to transport, quick to deploy and facilitates dense and specific survey patterns. Ten centimetres of depth is sufficient for the boat to manoeuvre, meaning that it can easily reach the ADCP's minimum depths of 18 cm for depth measurements and 30 cm for flow measurements. This is a major

benefit compared to a zodiac with an outboard motor, which requires deeper water to operate in. While flow measurements in very shallow water are not possible, the RCflow can easily gather bathymetric data in the shallows that can serve as reference data for modelling, or for interpolation purposes.

The RCflow is powered by a battery-powered model airplane motor that drives a propeller. The low-drag shape of the hull and the rather powerful motor allows the system to be operated in many flow conditions, although in flow exceeding 2 ms^{-1}, the batteries drain fairly rapidly. In those cases, if depth allows, a motor-powered zodiac with a tethered Hydroboard (Figure 10c) is preferable.

The remote controlled boat also allows for easy discharge measurements, without the need to tie a line across the stream to drag a Hydroboard back and forth or a manned boat to tether the sensor from (Yorke and Oberg, 2002). Therefore, a single operator can rapidly measure discharges for instance on rivers that would otherwise require a manned boat to cross and/or a second operator or some sort of rig to handle a line or rope for pulling the sensor across the stream. The RCflow makes it easy to manoeuvre smoothly and steadily at a slow pace so that idealised transects can be achieved with boat speeds below the local flow velocity in order to ensure the quality of the data.

4.1.2 Aerial photography

Regular aerial images used in Papers I and II were produced on July 4th 2005 by TerraTec AS and georectified by Norwegian Mapping Authority. The images were purchased as true colour RGB orthophotos at 8 bits per band at an 0.5 m spatial resolution. In Paper I the images covered 59 hectares in Garnjarga of river and in Paper II 42 hectares were covered near Tana bru.

In an effort to both increase the resolution of the bathymetric models and decrease or eliminate the time-gap between image acquisition and reference data acquisition, a UAV (Section 4.1.1.1) was used in Papers II and III to acquire low-altitude high-resolution aerial photography of the study area during the respective field campaigns. The cameras were set to automatically shoot one image every second. Camera focus was locked at infinity, white balance was fixed, aperture was f/5.6 with exposure times of 1/4000 s (2010) and 1/1000 s (2011) at ISO 800. Average flying height was 71.3 m (2010) and 127.5 m (2011). 60 x 60 cm^2 high-contrast ground control target points (GCP) were spread throughout the survey area and surveyed using RTK-GNSS. The images were mosaicked and orthorectified with a final ground resolution of 5 cm.

4.1.3 Bathymetry field data

The bathymetric modelling required reference depth measurements from the sites to be modelled. In Papers I and II, a Furuno FCV-600L dual frequency sonar with a ± 0.1 m accuracy was deployed form a zodiac, coupled with a Thales RTK-GPS system for positioning. The system sampled at ∼5 m intervals with a 5 cm positional accuracy. The sonar is able to measure depths of >0.6 m, leaving it unable to survey the shallows.

The shallow areas were surveyed with a pole-mounted RTK-GPS in Papers II and III. These river bed elevations were converted to water depths by subtracting the elevation from an RTK-GPS-based water surface interpolation.

A denser network of points was gathered using the vertical beam sonar on the Sontek M9 ADCP deployed on the RCflow (Papers II; III; IV). This system samples at 1 Hz and is able to survey the shallows down to 0.18 m and has an accuracy of 2.5 % of depth. The larger number of points that was gathered this way allows for better calibration and validation of the bathymetric models in Papers II and III and for the creation of bathymetric models as a direct interpolation of the surveyed points in paper Paper IV.

The shorelines were digitised manually based on the aerial imagery. These digitised polygons were used to both extract the water area from the images, since no infra-red band was available that would have allowed automatic extraction. The shoreline nodes thus created were converted to zero-depth samples. A subset of these that excluded non-river bed areas such as vegetation or shadows, was used in calibrating the bathymetric models.

4.1.4 Hydrological data

Hydrological data from the Finnish Environment Institute (SYKE) was utilised in order to adjust the depth values for each echo-sounded line to the water level of the date of the imagery acquisition flight (Papers I and II). Discharge data from the gauging stations in Utsjoki and Polmak were used in the calibration of the HAB bathymetry models (Paper I).

Water levels in Pulmanki were monitored during the study period using up to seven (depending on the year) water pressure loggers installed on the river bed throughout the study area (Solinst Levelogger Gold 3001), that, in combination with an air pressure logger allowed to derive water level changes at an accuracy of 0.3 cm. Actual water level elevations were measured at deployment time (in addition to later control measurements) using an RTK- or VRS-GNSS. This allows registering the water levels to the coordinate system as metres above sea level at a geographic location, rather than just as local depth.

4.1.5 Laser scanning

A range of methods were employed to survey the exposed, dry part of the river channel at high resolution in Paper III, including mobile laser scanning and terrestrial laser scanning.

In Paper III the ROAMER mobile mapping system (MMS) developed by the Finnish Geodetic Institute (FGI) is used for scanning the exposed topography of one meander bend of the Pulmanki river during two consecutive years. The ROAMER system can be applied both as a boat-based mobile mapping system (BoMMS) (Alho et al., 2009a; Vaaja et al., 2013) and cart/backpack-based MMS (AKhKA) (Kukko et al., 2012) (*cf.* Figure 11). At the time of measurement, this was likely the most advanced mobile laser scanning platform employed in fluvial studies.

The ROAMER MMS system consisted of a Faro Photon 120 laser scanner and a NovAtel SPAN navigation system with a NovAtel DL4plus GPS receiver, a NovAtel 702 GPS antenna and Honeywell HG1700 AG58 IMU integrated into a platform with

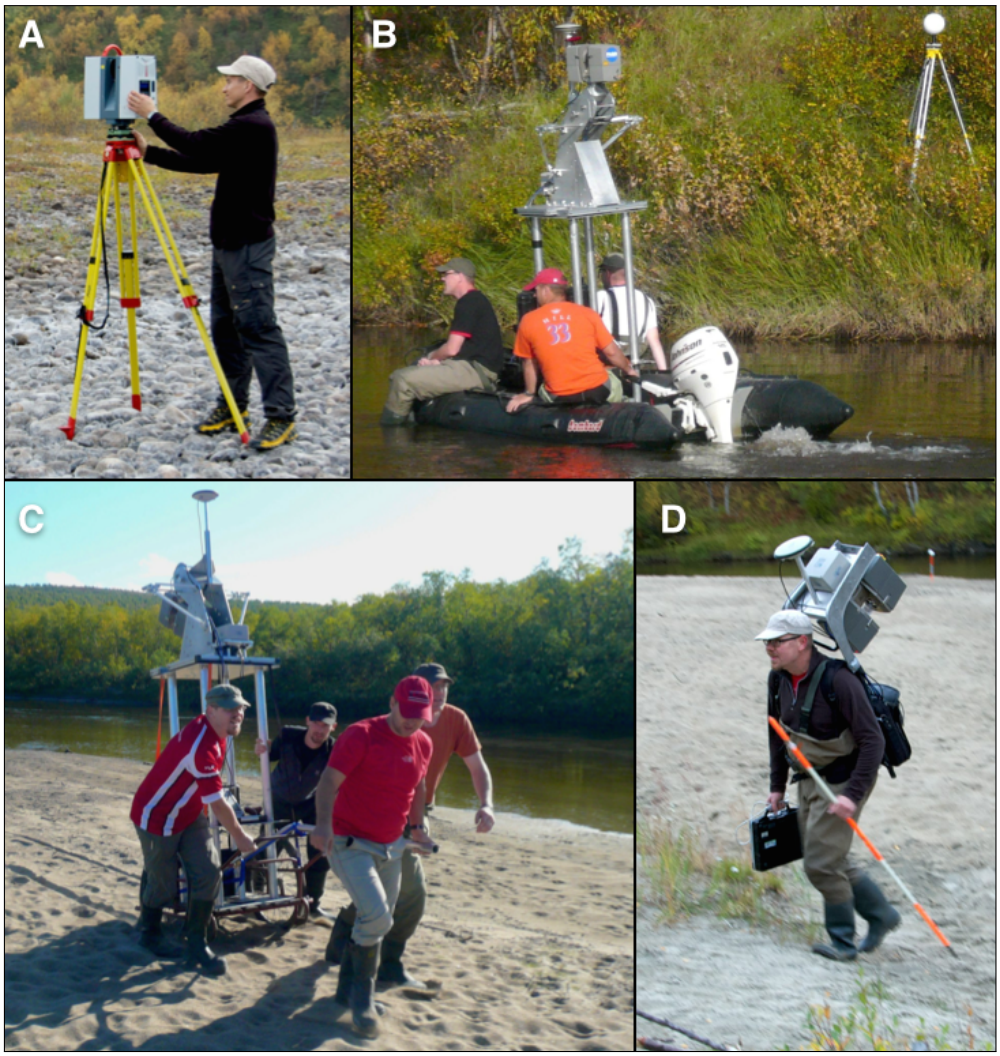

FIGURE 11 Laser scanning methods employed in this thesis: A. terrestrial laser scanning (TLS); B. the ROAMER system deployed on a boat (BoMMS); C. the ROAMER system deployed on a cart; D. Backpack based ROAMER system (AKhKA).

an adjustable scanning angle. The ROAMER MMS system was set up on a boat to collect laser scanning data of the point bar shoreline and the steep banks. The more elevated parts of the point bar were surveyed using the MMS mounted on a cart in 2010 and an more updated, lighter version (AKhKA) mounted on a backpack frame in 2011. Data of other parts of the point bars were collected using ROAMER installed on top of a cart.

All ROAMER surveys were conducted at a scanning frequency of 49 profiles per second yielding 244000 points per second. The profile spacing was 2–3 cm at an average speed of 4 km/h. The scanner field-of-view is 320 degrees, which means that with the scanner facing upwards on the boat installation, no data was acquired below the scanner, that is of the boat itself, and with the scanner facing downwards in case of the cart and backpack installations, the sky was not scanned.

Spherical reference targets set up throughout the survey area, the locations of which were measured by RTK-GPS, were used for registering the scans to the coordinate system (*e.g.* Figure 11B).

In addition to the mobile laser scanning data, terrestrial laser scanning (TLS) data was gathered as reference data using a used a Leica HDS6100 laser scanner (Paper III) (*cf.* Figure 11A). The point bar was scanned using TLS with a 360° horizontal field of view and a point spacing on the ground of 6 mm at a 10 m distance from the scanner. The same sphere reference targets as for MMS were used for orientating the scans to the coordinate system. The achievable accuracy of the RTK-GPS measurements is 1 cm + 1-2 ppm horizontally and 1.5–2 cm + 2 ppm vertically (RMSE) (Bilker and Kaartinen, 2001). The TLS is able to deliver millions of point measurements at the same level of accuracy as the RTK-GPS-measured target spheres, which makes this an ideal reference data set for all other topography data. TLS allows to gather a much more comprehensive reference data set compared to single RTK-GPS or Total Station points without compromising accuracy.

4.1.6 Acoustic Doppler Current Profiling

Flow field data was measured using a Sontek M9 ADCP deployed on RCflow (Section 4.1.1.2) with a Trimble R8 GNSS collecting precise positioning data (Figure 10a). In Paper IV a dense survey pattern was used to survey the 3D flow-field of one meander bend of the Pulmanki river. A Sontek S5 ADCP mounted on a Hydroboard floating platform tethered from a pole in front of a zodiac was used to survey a 3.5 km long reach of the same river over 4 days at a slightly less dense survey pattern (Figure 10d).

All ADCP surveys were carried out in discharge measurement mode using the ADCP's differential GPS (DGPS) for tracking. The DGPS uses the Satellite-based augmentation system (SBAS) to achieve sub-meter accuracy. Bottom tracking was not an option because of the mobile sandy river bed, especially during the spring flood.

4.2 Data processing and modelling

4.2.1 Modelling bathymetry

Three optical bathymetric models were tested in Paper I. The aim was primarily to test the newly developed hydraulically assisted bathymetry models (HAB) developed by Fonstad and Marcus (2005). These models (HAB1 and HAB2) presented the intriguing concept of optical bathymetry without the need for reference ground data collection in the field. These models were implemented in the R programming language (R Development Core Team, 2008) and evaluated against the more classical empirical Lyzenga model (Lyzenga, 1981). The HAB models were found to be able to produce a bathymetry model with absolute depth values given that Manning's roughness coefficient n is either known or correctly estimated. This roughness index is notoriously difficult to accurately estimate, however, and is generally calibrated in hydrodynamic models. While the absolute depth values of the HAB models are sen-

sitive to n, both HAB models were found to produce bathymetry of relative depths, which may be valuable for conducting change analysis using older images where ground data is not available.

The empirical Lyzenga linear transform model that is based on linearising the depth to image brightness ratio was calibrated using the depth-reference data (Section 4.1.3) (Papers I, II, III). The model is calibrated by performing a deep water correction and regressing these corrected values to the image brightness values for the red and green bands. Paper I uses this basic method, while Paper II introduces an algorithm for estimating the deep water correction variable that is often impossible to determine empirically in rivers. In Paper I the data was split into a calibration and a reference set, whereas in Papers II and III k-fold random subsetting cross-validation was used for achieving unbiased estimators of both the the linear regression coefficients for calibration and for the accuracy assessment.

The modelling process is the same for the high-altitude aerial image-based models (Papers I and II) and the UAV-based models (Papers II and III)

In Papers I and II the bathymetric models were literally depth models, whereas in Papers III and IV the depth models were converted to river bed elevation models by subtracting the modelled depths from a RTK-GNSS-based water surface, similar to *e.g.* Williams et al. (2011) and Javernick et al. (2014).

In Paper IV, the bathymetry model was produced as an interpolation of the bed elevations of the densely surveyed ADCP points. The bed elevations were computed as a side-product of the 3D flow field point cloud by subtracting the ADCP-measured water depth from the water surface elevation.

4.2.2 Seamless wet-dry topography

Paper III merges a UAV-imagery based bathymetric model with MMS-based LiDAR topography. The mobile LiDAR data are composed of BoMMS and CartMMS or AKhKA-gathered point clouds. The point clouds were referenced to tripod-mounted target spheres that were surveyed using RTK-GNSS. The referenced and merged point clouds were filtered according to the method developed by Axelsson (2000). The algorithm classifies terrain points by starting with a few seed points that are likely ground hits and iteratively builds a triangulated surface, starting with the lowest points and adding more points from the data set to the surface based on given thresholds of maximum angle to the triangle surface and maximum distance to the triangle edges that contain the points. More points are added this way until no more points are left that fall within the given thresholds.

In order to merge the UAV-photography-based river bed elevation data with the mobile LiDAR point cloud, the depth raster was converted to a regular point cloud with one point for each raster pixel centre. The shoreline for merging the data sets was determined using the intensity values of the LiDAR points. The near-infrared LiDAR (785 nm) gets absorbed rapidly by water, but some points were registered in the very shallow areas. The intensity of these points was found to be a very useful indicator of the shoreline (Vaaja et al., 2013) and utilised in subsetting both datasets. After adjusting any systematic error in the river bed elevation model to the more precise LiDAR model, a seamless wet-dry topographic model was created containing the river bed and the floodplain in one digital elevation model (DEM).

4.2.3 Modelling 3D water flow

The dense zig-zag pattern ADCP data was converted to a 3D point cloud of flow vectors in Paper IV. The 1 Hz ADCP samples were merged with 10 Hz VRS-post-processed RTK-GNSS positions using GPS time stamps. The position for each individual ADCP cell (bin) of each ADCP sample (ensemble) was calculated and merged with the respective flow velocities and directions, local water surface and depth to yield a point cloud of flow and topography, all in one data set. These raw data can be used to interpret the 3D flow field by visualising flow velocities or directions. The river bed and the water surface can be interpolated from the point cloud data to add to the visualisation and support interpretation of the data. The raw, irregularly space point cloud was subsequently interpolated in 3D into a regular matrix. This has the benefit of simplifying the data so that interpretation is easier. In particular the regular nature of the matrix makes it possible to interpret the data as virtual transects. Furthermore, the interpolation serves as a low-pass filter on the flow data and the regular matrix makes it possible to analyse the flow data as estimates of volumes. It is now possible to analyse the total volume of water in a given reach, as well as a spatial volumetric flow distribution, that is, it can be analysed how much water moves at what velocity and where.

5 RESULTS AND DISCUSSION

5.1 Bathymetric models

Papers I and II investigate different aspects of optical bathymetric models. The HAB 1 and HAB 2 models that are based on hydraulic theory for their calibration are evaluated against the widely used Lyzenga model that requires ground measurements of reference depth points to be calibrated. Additionally, the optical models are compared to an interpolation of sonar points. All three remote sensing based models were able to produce a spatially continuous surface of depth values that, from a visual analysis, compare favourably to the interpolation model. However, as Marcus et al. (2012) put it: "just because it looks good, does not mean that it is good". On the other hand, the same authors (Fonstad and Marcus, 2005) and later Walther et al. (2011) also found a visual appraisal of a model to be of great importance and possibly as telling as certain statistical indicators, referring specifically to bathymetric models. The work presented in this thesis indicates that both the statistical analysis, generally expressed in terms of root mean square error (RMSE), and a visual assessment, both in terms of the bathymetric maps and the analysis of transects is important in the evaluation of the quality of a remote sensing based bathymetric model.

The HAB models both underestimated the river depths when compared to the sonar reference points. Their main problem was found to be the sensitivity to the estimation of the Manning's roughness coefficient n. The hydraulic equations that are used in the calibration of the model hinge on this parameter, which is very difficult to estimate reliably (Wohl, 1998). Generally, in hydraulic modeling, roughness is calibrated by adjusting it to yield a known discharge at a known stage. Stage being equal to water depth, we can not calibrate n since we don't know depth when modelling bathymetry. Fonstad and Marcus (2005) used Jarrett's (1984) equation to determine n in high gradient streams, whereas a previously calibrated n was used in Paper I as well as two larger coefficients for testing the model's response to variation in n. Both HAB models were found to be equally sensitive to n, reaching the mean and maximum measured depths only at an n value of 0.005. This means that, unless one can be confident in the roughness coefficient employed, one can not know the

quality of the depth values modelled with the HAB models without ground values to check them against. Jarrett (1984) found the average standard error of their estimation method to be 28% based on their test data, leaving a corresponding uncertainty in the bathymetric models when relying on this estimator.

The HAB 2 model was also evaluated in terms of the wet shore pixel selection method. Fonstad and Marcus (2005) suggested two methods for determining this value, one based on manual selection of wetted shore pixels and the other an automatic selection of the brightest pixels in the cross-section used for calibration. Both methods were tested and found to lead to differing results, with the automatic method leading to a greater depth spectrum modelled than the manual selection. These two methods are not interchangeable. Based on the results of Paper I the automatic selection method seems to be preferable because it achieves a depth distribution closer to that measured, with identical r^2 and RMSE values.

Out of the two HAB models, HAB 2 was found to be the more promising. This model calculates depth by trying to estimate the attenuation coefficient of light in the water column, and therefore is based on fewer assumptions than the HAB 1 model that assumes a symmetric frequency distribution of depths in the cross-section of the channel. HAB 2 was also evaluated by Walther et al. (2011) in a gravel bed river in Oregon, USA, and they achieved r^2 values between 0.52 and 0.89 using different image sets. This metric however only indicates the level of fit of the model, which is important, but does not reveal error in terms of vertical distance, and they did not calculate RMSE despite having sonar ground measurements available. Walther et al. (2011) is the only study apart from Paper I to have evaluated HAB models after their initial publication, but their results are hard to compare to the ones in Paper I due to the nature of their evaluation. While it would be very useful to have a truly remote sensing based optical bathymetry modelling method, in the sense of it not requiring ground data for calibration, the HAB models have their limitations as far as absolute depth values are concerned. They are however likely very useful in modelling bathymetry based on historic imagery, which would not be possible with an empirically based method. Lane et al. (2010) worked in the same direction, using photogrammetry on historical aerial photographs. The HAB 2 model would be particularly usefully applied on historic image data if the channel roughness could be estimated from the present situation and assumed not to have changed much over time. This would require a measurement campaign in the field though.

Paper I also evaluates the empirical Lyzenga model, using deep water radiance values sampled from a deep section of the Tana River in Tana Bru. Lyzenga's (1981) model performs better than the HAB models, with an r^2 of 0.95 and an RMSE of 0.13 m when considering the whole study area. While the red band HAB models are able to produce similar RMSEs, the Lyzenga model replicates the minimum, mean, and maximum depths more faithfully than the other models.

The study area in Garnjarga (Paper I) contained an area of algae covered rocks that violate the uniform substrate assumption of all the bathymetric models used, leading to and overestimation of depth in this area and highlighting the importance of keeping with the assumptions of the models in question, regardless of the model type. All models performed best using the red and green bands, which is in line with the findings of Winterbottom and Gilvear (1997) and (Legleiter et al., 2009) and Walther et al. (2011).

Paper II focussed further on the Lyzenga model. This is based on the findings of Paper I. Since it does not seem possible to determine water depths with any amount of certainty without ground data, and since ground data is in any case necessary for accuracy assessment, an empirical model may as well be used. The deep water radiance estimation algorithm presented in Paper II was shown to deliver results similar to those that could be manually digitised in the deepest pool of the Tana River, near Tana Bru. Having an estimator for this variable makes the Lyzenga model more readily applicable to shallow streams and it was concluded that even in rivers deep enough to manually digitise deep water radiance, an objective estimator may be in any case preferable to a subjective manual process. The estimator also revealed that, in optically shallow streams, deep water radiance may be negligible. While this may be so, there is no harm in using the estimation algorithm, especially considering that there is likely no clear line determining whether or not it is safe to ignore deep water radiance.

Paper II also showed that there is a limit beyond which optical depth estimates are no longer reliable, even if the river bed may still be visible. In the case of Tana Bru, depths beyond half Secchi depth could not be modelled successfully. Walther et al. (2011) also found depths beyond 1.5 m not to be accurately modelled, and they draw the same conclusion as Paper I that this is reaching a limitation beyond which the signal is no longer entirely, or rather predominantly, a function of depth (Legleiter et al., 2004).

Paper II presented one of the first cases of an optical bathymetric model that was constructed from UAV-based orthoimagery, leading to a very high spatial resolution of 5 cm ground pixel size. This technique was also employed by Zinke and Flener (2013) and (Tamminga et al., 2014) as well as in Paper III.

5.2 Topographic models

In an effort to get a more holistic view of river environments Paper III merges optical bathymetric modelling with mobile laser scanning and UAV photogrammetry to create a seamless DTM. Modelling was conducted during two consecutive years in order to be able to assess the method for its ability to conduct change detection in river environments. All non-bathymetric topography was evaluated against TLS point clouds. TLS achieves the accuracy of the RTK-GPS used to survey the calibration targets and at the same time offers a spatial coverage and measurement density at an accuracy that would be inconceivable with other methods. In practical terms, TLS produces a DTM that is the closest thing to the true surface that can be reasonably achieved. UAV photogrammetry produced DTM point clouds with an accuracy of between 0.1 and 0.15 m relative to TLS, depending on the input images. The ground resolution and uniformity of flying height and flight pattern had a positive effect on the accuracy of the point cloud produced. MLS, a combination of BoMMS and CartMMS in 2010 and BoMMS and AKhKA in 2011 achieved accuracies better than 0.02 m with reference to TLS. These data were combined with the UAV-based optical bathymetry, using Lyzenga's (1981) algorithm in combination with the deep water radiance estimation presented in Paper II. The bathymetric model produces sub-decimetre accuracy in

terms of pure depths, but the accuracy of the depths converted to elevation to produce a DTM that could be combined with other DTM data into a seamless model of riverine topography, depends on the accuracy of the water surface measurements and interpolation model. The data was merged by finding the edge of the water using the abrupt intensity gradient in the laser scanning data that had been noted in Vetter et al. (2011) and Vaaja et al. (2013). Both the bathymetry DTM and the MMS DTM were were clipped using this water polygon and then merged. The resulting seamless DTM presented a smooth surface, when analysed in transect form and gives a good synoptic view of the whole active channel, including the low water channel and the flood plain, as well as the immediate riparian area.

The seamless DTMs of two consecutive years were used for detecting changes by calculating a DTM of difference (DoD). The level of detection (LoD) — an indicator of what changes are real at a given confidence interval, beyond the uncertainty in the models (Milan et al., 2011)— was calculated based on the accuracy of the DTMs. The overall vertical accuracy defaults to the lowest level of the DTMs, in this case the bathymetry. Because the level of accuracy achievable under water is one order of magnitude lower than the one on dry land, the LoD values were analysed for the wet and dry part separately. Since the LoD accounts for cumulative error in different DTMs, the order of magnitude difference between wet and dry areas is reflected in this statistic as well with the dry area having a LoD of 0.045 at a 95% confidence interval, and the bathymetry as well as the photogrammetry point cloud exhibiting ten times that. Prior to this work, change detection had only been carried out on either the dry or the submerged parts of the channel (*e.g.* Alho et al., 2011a). More recently Tamminga et al. (2014) merged wet and dry topography into a seamless model as well.

It was concluded that it is possible to create a seamless wet-dry topography of river environments using a combination of methods, and that, indeed, there are several options for achieving this. Given that the optical bathymetric model requires aerial images, the simplest and most economical way to create a seamless DTM would be to combine the UAV point cloud with the bathymetric model. Based on the results of Paper III this leads to a model with more or less uniform error of around 10 cm, which is adequate for many applications, such as hydraulic modelling, change detection of larger areas, or habitat modelling, to name a few. In case a higher level of accuracy is required, such as small scale change detection, MLS provides the answer, but at a higher cost. Beyond the findings of Paper III it can be noted that the rapid pace of development in photogrammetry, notably with the method of structure-from-motion DTM generation (Fonstad et al., 2013; Vaaja et al., 2011b) and the low requirements as far as camera equipment goes, may result in UAV-imagery based DTMs that approach the level of accuracy of MLS in the near future. Some research is also looking into the possibility of creating the underwater topography directly from photogrammetry by correcting the refraction of the light at the air-water boundary (Murase et al., 2008). Topography points determined by photogrammetry — or laser scanning — that lie underwater are not modelled correctly, unless the refraction of the light beam at the water surface is corrected for in a manner that accounts for the continuously varying angle of the beam to the sensor throughout the area captured. This was not attempted in the present study.

Furthermore, the possibility of combining dry topography data with bathymetric data gathered by an ADCP, such as in Paper IV also needs to be considered, if

available. The ADCP based depth model has the benefit of being independent of river bed sediment, but more importantly does not require the bed to be visible, meaning that it can be used in turbid water or water too deep to model with optical methods. Compared to an optical model that is based on an image that covers the surface to be modelled in a contiguous manner and therefore the resulting bathymetric model is also based on measured values for the whole area, the ADCP based bathymetry is based on an interpolation of measured depth points, and is therefore reliant on the density of the sampling pattern for a realistic model to be produced.

5.3 Multidimensional flow field models

Paper IV presents a new method of capturing the 3D flow field in 3D space using an ADCP mounted on a remote controlled boat in combination with a kinematic GNSS positioning (RCflow). The flow field is surveyed in a zig-zag pattern and the positions for each flow measurement sample are recorded. After merging the ADCP data with the positioning data, the precise position of each cell in each sample can be determined, so that each 3D flow vector consisting of directional magnitudes — that is flow velocity to the north, the east and upwards (ENU) — can be positioned in 3D space with XYZ coordinates in a geographic coordinate system. This results in a point cloud of flow vectors that represent a time-integrated snapshot of the surveyed flow field. The 3D cloud of flow vectors can be further processed into a 3D matrix to create a regularly spaced cloud of flow vectors. This allows the calculation of flow volumes in the study area, that is the total volume of water, as well as the volumetric flow distribution. This was not possible before. Tsubaki et al. (2012) presented a new interpolation method for unstructured 3D flow field data recently, but rather than a point cloud, they create flow layers. Laamanen et al. (2014) also presented a method for analysing areally gathered unstructured flow field data in terms of either depth-averaged flow or top or near-bed layers. This is indeed a derivative of the method presented in Paper IV. Tsubaki et al.'s (2012) method differs in that it creates layers throughout the water column. The matrix data in Paper IV could also be analysed as a stack of layered flow fields.

Areal 3D flow field data was gathered on nine days during the snow-melt induced spring flood on the Pulmanki River in May 2013. A 3.5 km reach was surveyed in a relatively coarse zig-zag pattern and the same meander bend that was studied in Papers II and III was surveyed in detail with a very dense survey pattern. The 3D flow point cloud allows the detection of the high velocity core (HVC) as well as flow directions revealing back-flow eddies for instance. The time series of flow point clouds at the meander bend study area makes it possible to follow the evolution of the flow pattern, in particular the location and shape of the HVC, as the water rises to inundate the point bar. While the HVC is detectable along with vertical flow patterns that indicate overturning flow as would be expected in a meander bend (Section 2.2.1) the patterns are not as clearly defined as the theory might suggest. This may be due to the fact that the theory is a simplified concept of reality, but it may also be due to noise in the flow measurement data. While the field site in Pulmanki is on the whole a good site to survey with an ADCP, this does not mean that all as-

sumptions inherent in ADCP measurements (Section 2.2.3) are at all times met. In particular, the assumption of horizontal homogeneity of flow between all beams is unlikely to hold at all times during the measurement (Rennie, 2008). Measurement errors may also be introduced through compass errors or alignment errors or ADCP positioning errors with reference to the flow vector. Zhao et al. (2014) recently introduced a method for mitigating the alignment errors in a way that may reduce flow velocity estimate errors from 0.3 ms^{-1} to 0.02 ms^{-1}.

When considering the whole flow field though, it is relatively easy to ignore noise in the data and gain an unprecedented insight into the areal flow patterns in 3D. These data may be processed further to analyse other hydraulic variables. The point cloud flow data contain all the information necessary to calculate local stream power (Equation 5) which can be related to bed morphology. As a side effect of producing the point cloud, a bathymetric model can also be produced, which, as mentioned above could be merged with other DTM data. Laamanen et al. (2014) analyse the influence of spatial variability of stream power on changes in bed morphology over the same flood period.

5.4 Combining all models to a unified river model

The work presented in the original papers of this thesis can be combined to yield a unified model of hydromorphology: the seamless topography of Paper III, based on the findings of Papers I and II, forms the riverscape through which the 3D water column modelled in Paper IV flows and on which it has a shaping effect all the while being affected by it. An exemplary representation of such a model is shown in Figure 12, consisting of the optical bathymetry/MMS seamless DTM of 2011 with the flow field of May 19. 2013 superimposed. As was discussed above, there are a variety of methods that can be used to achieve this, based on the ones presented in this thesis, as well as others, that were not included, such as swathe sonar (Horritt et al., 2006), aerial LiDAR (Bailly et al., 2012), or green LiDAR (Kinzel et al., 2013) for instance.

Where a unified river model is to be built, there is usually a requirement for at least two remote sensing methods that need combining. A mobile ADCP with an accurate positioning system is essential for mapping the flow field. There is at present no other method that can truly be used as a substitute. Depending on the intended use of the data, say mapping potential spawning grounds of salmon, the ADCP may provide all there is needed, since the riparian area and the flood plain are not of interest in that case. The flow field can be mapped along with the riverbed topography using this one measurement set-up. In fact, when mapping during a flood event, which, in the case of many sub-Arctic river systems consists of a fairly predictable snow-melt flood, the flood plain and its flow field can also be mapped, bar the very shallow areas near the shore, using the ADCP (Paper IV). The remote controlled ADCP system allows for more detailed manoeuvrability compared to a system tethered from or mounted to a regular boat. One major advantage of this system, in addition to it's ease of deployment, is its ability to map shallow areas down to the limits of the ADCP sensors.

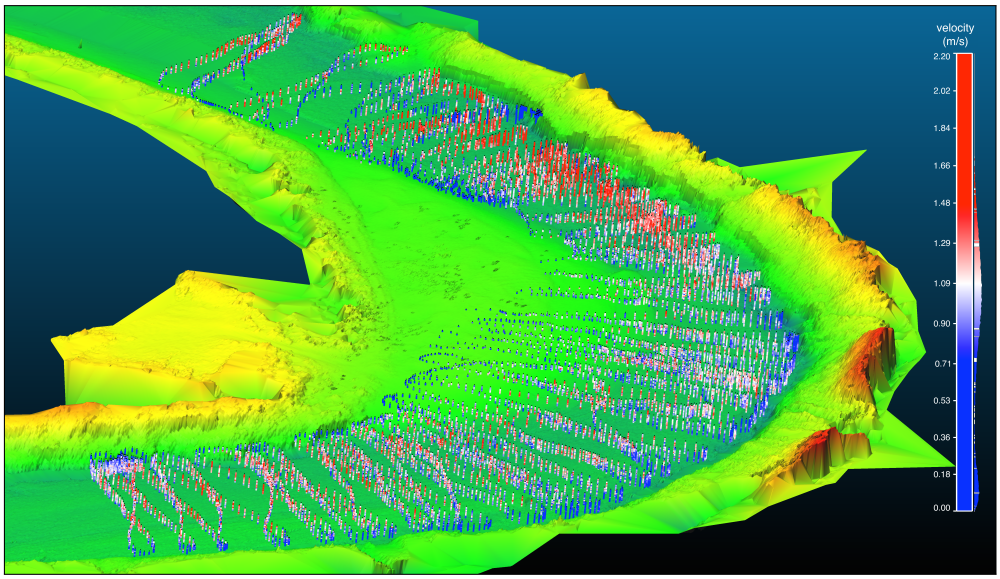

FIGURE 12 Unified 3D hydrographic model, combining the seamless topography created by merging mobile laser scanning with UAV-based optical bathymetry modelling with the RCflow-based 3D flow point cloud. This example shows flow data during the spring flood inundating the point bar with point colour representing flow velocity in m/s.

As soon as the food plain or other riparian areas are to be included in the model, however, another method is required to map the exposed topography. In many cases, mobile laser scanning is a great solution since it allows to map fairly large areas at great precision in a short amount of time, from a point of view that captures the river banks better than aerial LiDAR. In rivers with wide open flood plains and no steep banks, aerial LiDAR may be an excellent option, which, nowadays is also becoming more widely available as readily scanned and processed and possibly, depending on location, freely available data.

In case the requirements demand that the model depict a specific period of time, such as a flood event, these readily available data are no longer applicable and mobile laser scanning represents a more versatile, and likely cheaper option, since it does not require the use of a dedicated survey airplane. TLS is also an option for smaller areas and it will deliver good results, but it is relatively slow compared to other remote sensing methods. Clearly, compared to surveying topography points with a pole-mounted GNSS or total station, TLS is markedly faster and will cover more area at a higher density than non-remote sensing methods. Williams et al. (2013a) mounted a TLS system to an amphibious all-terrain vehicle in order to cover a larger area faster with this system. This is a semi-mobile system in the sense that the scanner is not mounted on a stationary tripod, but the scans are performed in stop and go mode, not while the vehicle is moving. Another option becoming available as scanners get smaller and battery technology improves, is to mount a laser scanner on a UAV (Jaakkola et al., 2010; Glennie et al., 2013).

On the other hand, the camera-based UAV surveys that have been performed in the present work present a great opportunity for flexibly mapping river environ-

ments at the reach scale, covering both the riparian area and, in rivers with clear water that is optically shallow, the channel, using structure-from-motion based point clouds and optical bathymetry. This is probably the most economical method of hydromorphological mapping, in combination with the ADCP, as the hardware requirements are low since the point cloud quality is more dependent on the shear number of images and their relative view angles than the specifications of the camera systems, to the point that even mobile phone cameras are being investigated for mapping purposes (Micheletti et al., 2014; Tamminga et al., 2014). It will be most interesting to see where advances in this space will take photogrammetry relative to laser scanning for reach scale topographic mapping in the future.

5.5 Directions for future research

There remains a gap in the vertical accuracy between dry topography and bathymetry that needs to be shrunk. This remains a challenge, even in clear water. Acoustic methods are limited in the shallows and optical methods are limited not just by turbidity, but also the refraction of light on the water surface. Hopes have been high for a while already that green LiDAR may provide the answer to this problem, but thus far, results from green aerial LiDAR have not been very encouraging in river environments, mainly due to the increasingly large footprint of the laser beam under the water. New developments in laser scanning technology leading to mobile green or multispectral LiDAR may open new possibilities in remote sensing of bathymetry in rivers. The rapid progress in photogrammetry bay also open new possibilities for remote sensing of bathymetry. Perhaps structure-from-motion technology with a surface refraction correction may provide one answer.

Another topic that will be of interest is the analysis of the spatial distribution of errors, both in the bathymetric and the flow model. While the spatial error distribution of DTM has been investigated (*e.g.* Oksanen, 2006), similar studies of bathymetry in rivers, in particular relating to optical bathymetry, are still lacking. Given the novelty of the methodology, the same is true for the 3D flow model. In fact, determining the spatial error distribution of this type of model should represent quite a challenge due to the extra dimension. The quantification of a benchmark for 3D flow models is also interesting.

The methods developed in the present thesis can be employed to gain a better understanding of fluvial processes. The integrated hydromorphological model methodology can be used to gain insights into the patterns and interconnections of flow and channel processes and their spatial interconnections. In particular, multitemporal data, preferably over longer sections of river would be useful to this end. Williams et al. (2015) are already working in this direction, although the 3D flow model may enhance future studies of this type. The hydromorphological model consisting of wet-dry topography and the three-dimensional flow filed can be used to

investigate for example the evolution of meander bends or braiding in natural rivers, but also the scouring and deposition around engineering structures such as bridges or dams. Another interesting avenue of research would be to validate 3D hydraulic models using the measured 3D flow model presented in this thesis.

The applicability of the 3D flow model on longer reaches may be enhanced by further improving the vertical positioning of the flow measurement system and investigating methods of dynamic water surface interpolation.

The hydromorphological model can still be enhanced by adding further quantification of fluvial processes, such as the investigation bed material mobilisation and stability. Some work has already been conducted on measuring sediment transport using ADCP bottom track bias for instance (*e.g.* Rennie and Church, 2010) that may be incorporated into the hydromorphological model. Another aspect that would be very useful to integrate into the model would be the characterisation of bed material type or roughness.

The high resolution bathymetry that can be achieved using UAV photography, combined with the temporal flexibility it allows, opens up the possibility for studying fine scale fluvial processes, such as the dynamics of dunes on sandy river beds. The areal 3D flow mapping combined with high resolution bathymetry allows for more detailed study of the connection between process and form in river environments.

6 CONCLUSIONS

This study contributes to the advancement of hydromorphology by combining and developing different surveying and modelling methods to create a unified river model of topography and water flow field. Empirical optical bathymetric modelling was developed further, after an evaluation of theoretically based vs. empirical models had been performed. The thus developed empirical model was combined with close-range mobile mapping methods to produce a seamless riverine topography, which forms the basis for the three-dimensional empirical water flow field model to be situated on. The main conclusions and advancements of this thesis are the following:

1. Optical bathymetric modelling was found to be a feasible and useful method in clear sub-Arctic rivers. The theoretical hydraulically assisted bathymetry models (HAB) were found to produce plausibly looking models of underwater topography that are however reliant on the correct estimation of Manning's roughness coefficient. If this parameter can be reliably estimated in some other fashion, the HAB 2 model in particular may be useful, especially since it can be applied to historical images. Lyzenga's (1981) empirical model was found to deliver sub-decimetre accuracy if the model assumption of substrate uniformity is not violated.

2. It was established that the deep water radiance variable in Lyzenga's linear transform equation can be reliably estimated, even in rivers too shallow for it to be directly determined from the image data. Furthermore it was concluded that in very shallow rivers, it may be safe to ignore deep water radiance in Lyzenga's (1981) model. Nevertheless, since it is hard to predict how much or little this variable affects the model in any given situation, it was concluded that it may as well be estimated. The automatic estimation also provides a previously unavailable objective method for estimating deep water radiance in deeper water, possibly in coastal waters too, where it can not be ignored.

3. A seamless river environment topography was constructed by merging optical bathymetry with mobile laser scanning. High-resolution bathymetry was created using UAV images and a sub-decimetre vertical accuracy was achieved in

a sandy bed river. The same images were used to create a point cloud of the dry topography, with the same level of accuracy as the underwater topography. A combination of boat- cart- and backpack-based mobile laser scanning resulted in a DTM of the exposed channel and adjacent riparian area of better than 2 cm accuracy. This MLS model was merged with the bathymetric model to create a seamless wet-dry topography. The merging of these models was found to work well. Seamless models of two consecutive years were used for a seamless change analysis by means of a DoD. The evaluation of the DoD was concluded to be best performed by considering the differences in LoD for the different measuring methods.

4. A new methodology for modelling and visualising the 3D flow field in 3D space at the reach scale was presented. It was demonstrated that it is possible to capture the flow of a river at the reach scale into a 3D point cloud of flow vectors that allows the detection of spatial flow patterns. An interpolation of the raw measured flow vectors into a 3D matrix, in addition to providing spatial averaging, makes it possible to quantify volumetric flow. The utility of the method was showcased by demonstrating how the changes in the flow field can be monitored in 3D over the period of a spring flood, for instance by tracking the high velocity core. The potential for further development of this empirical flow modelling methodology, for deriving other hydraulic parameters in a spatial manner, was noted as well.

5. The combined work of this thesis yields a unified model of hydromorphology based entirely on field-measured data. The 3D water flow field model can be superimposed onto the 3D seamless topography to give comprehensive picture of the fluvial environment. This kind of perspective on rivers has thus far not been possible based on measured data.

The combination of methods presented and used in this thesis, or a subset thereof, as discussed, can produce a synoptic model of river hydromorphology that should be able to support many fields of research such as, hydrology, fluvial geomorphology, hydro-ecology as well as integrated river management.

REFERENCES

Alaraudanjoki, T., Elster, M., Fergus, T., Hoset, K. A., Moen, K., Rönkä, E., and Smith-Meyer, S., 2001: Tenojoen eroosio, Tenojoen säilyttäminen luonnontilaisena lohijokena, Raportti A Eroosion ja sedimentin kulkeutuminen, Tech. Rep. Tnro 1399R0004, Lapin ympäristökeskus.

Alho, P. and Mäkinen, J., 2010: Hydraulic parameter estimations of a 2D model validated with sedimentological findings in the point bar environment, Hydrological Processes, 24, 2578–2593, doi:DOI 10.1002/hyp.7671.

Alho, P., Kukko, A., Hyyppä, H., Kaartinen, H., Hyyppä, J., and Jaakkola, A., 2009a: Application of boat-based laser scanning for river survey, Earth Surface Processes and Landforms, 34, 1831–1838, doi:10.1002/esp.1879.

Alho, P., Mäkinen, J., Lotsari, E., Flener, C., and Käyhkö, J., 2009b: Flow parameter estimations of a two dimensional hydraulic model validated with sedimentological findings, in Change - Society, Environment and Science in Transition., Turku University Department of Geography Publication B Nr 14, 3rd Nordic Geographers Meeting, 8.–11. June 2009, Turku, Finland.

Alho, P., Vaaja, M., Kasvi, E., Kukko, A., Hyyppä, H., Hyyppä, J., Kaartinen, H., Kurkela, M., and Flener, C., 2011a: Multitemporal MLS data and terrestrial photogrammetry in a change detection of point bars, in Geophysical Research Abstracts, vol. 13, European Geosciences Union, Vienna, Austria.

Alho, P., Vaaja, M., Kukko, A., Kasvi, E., Kurkela, M., Hyyppa, J., Hyyppa, H., and Kaartinen, H. a., 2011b: Mobile laser scanning in fluvial geomorphology: mapping and change detection of point bars, Zeitschrift für Geomorphologie, 55, 31–50, doi:http://dx.doi.org/10.1127/0372-8854/2011/0055S2-0044.

Anandakumar, R., Milton, E., and Sear, D., 2008: River habitat mapping using Airborne Imaging Spectrometry (CASI-2), in Proceedings of the Remote Sensing and Photogrammetry Society Conference: "Measuring Change in the Earth System", vol. 1-4, University of Exeter, Remote Sensing and Photogrammetry Society, Nottingham, UK.

Anderson, M. G., Bates, P. D., et al.: Model validation: perspectives in hydrological science., John Wiley & Sons Ltd.

Axelsson, P., 2000: DEM generation from laser scanner data using adaptive TIN models, International Archives of Photogrammetry and Remote Sensing, 33, 111–118.

Bagnold, R., 1966: An approach to the sediment transport problem from general physics, US Geol. Surv. Prof. Pap., 422, 1, 231–291.

Bailly, J.-S., Kinzel, P. J., Allouis, T., Feurer, D., and Le Coarer, Y.: Airborne LiDAR Methods Applied to Riverine Environments, pp. 141–161, John Wiley & Sons, Ltd, doi:10.1002/9781119940791.ch7.

Bates, P., 2004: Remote sensing and flood inundation modelling, Hydrological Processes, 18, 2593–2597, doi:DOI 10.1002/hyp.5649.

Bates, P., Horritt, M., Smith, C., and Mason, D., 1997: Integrating remote sensing observations of flood hydrology and hydraulic modelling, Hydrological Processes, 11, 1777–1795.

Bates, P., Marks, K., and Horritt, M., 2003: Optimal use of high-resolution topographic data in flood inundation models, Hydrological Processes, 17, 537–557, doi:DOI 10.1002/hyp.1113.

Bates, P. D., Lane, S. N., and Ferguson, R. I.: Computational fluid dynamics: applications in environmental hydraulics, J. Wiley, Hoboken, NJ.

Bathurst, J. C., Hey, R. D., and Thorne, C. R., 1979: Secondary flow and shear stress at river bends, Journal of the Hydraulics Division, 105, 1277–1295.

Bilker, M. and Kaartinen, H., 2001: The quality of real-time kinematic (RTK) GPS positioning, Reports of the Finnish Geodetic Institute, 2001:1.

Birkinshaw, S., O'Donnell, G., Moore, P., Kilsby, C., Fowler, H., and Berry, P., 2010: Using satellite altimetry data to augment flow estimation techniques on the Mekong River, Hydrological Processes, 24, 3811–3825.

Brakenridge, G. R., Nghiem, S. V., Anderson, E., and Chien, S., 2005: Space-based measurement of river runoff, Eos, Transactions American Geophysical Union, 86, 185–188.

Brasington, J., Rumsby, B., and McVey, R., 2000: Monitoring and modelling morphological change in a braided gravel-bed river using high resolution GPS-based survey, Earth Surface Processes and Landforms, 25, 973–990.

Bryant, R. G. and Gilvear, D. J., 1999: Quantifying geomorphic and riparian land cover changes either side of a large flood event using airborne remote sensing: River Tay, Scotland, Geomorphology, 29, 307–321.

Bukata, R. P., Jerome, J. H., Kondratyev, A. S., and Pozdnyakov, D. V.: Optical properties and remote sensing of inland and coastal waters, CRC press.

Bull, W. B., 1979: Threshold of critical power in streams, Geological Society of America Bulletin, 90, 453–464.

Carbonneau, P., Dugdale, S., and Clough, S., 2010: An automated georeferencing tool for watershed scale fluvial remote sensing, River Research and Applications, 26, 650–658.

Carbonneau, P., Fonstad, M. A., Marcus, W. A., and Dugdale, S. J., 2012: Making riverscapes real, Geomorphology, 137, 74–86.

Carbonneau, P. E. and Piégay, H.: Fluvial Remote Sensing for Science and Management, John Wiley & Sons, Ltd, doi:10.1002/9781119940791.

Carbonneau, P. E., Lane, S. N., and Bergeron, N. E., 2004: Catchment-scale mapping of surface grain size in gravel bed rivers using airborne digital imagery, Water resources research, 40.

Carbonneau, P. E., Bergeron, N., and Lane, S. N., 2005: Automated grain size measurements from airborne remote sensing for long profile measurements of fluvial grain sizes, Water Resources Research, 41.

Carbonneau, P. E., Lane, S. N., and Bergeron, N., 2006: Feature based image processing methods applied to bathymetric measurements from airborne remote sensing in fluvial environments, Earth Surface Processes and Landforms, 31, 1413–1423, doi:DOI 10.1002/esp.1341.

Castillo, E., Pereda, R., Manuel de Luis, J., Medina, R., and Viguri, J., 2011: Sediment grain size estimation using airborne remote sensing, field sampling, and robust statistic, Environmental Monitoring and Assessment, 181, 431–444, doi:DOI 10.1007/s10661-010-1839-z.

Chandler, J. and Moore, R., 1989: Analytical photogrammetry: a method for monitoring slope instability, Quarterly Journal of Engineering Geology and Hydrogeology, 22, 97–110.

Chandler, J., Lane, S., and Shiono, K., 1998: Acquisition of digital elevation models at high spatial and temporal resolutions using automated digital photogrammetry.

Chandler, J., Ashmore, P., Paola, C., Gooch, M., and Varkaris, F., 2002: Monitoring river-channel change using terrestrial oblique digital imagery and automated digital photogrammetry, Annals of the Association of American Geographers, 92, 631–644.

Charlton, M. E., Large, A. R., and Fuller, I. C., 2003: Application of airborne LiDAR in river environments: the River Coquet, Northumberland, UK, Earth surface processes and landforms, 28, 299–306.

Cho, H. J. and Lu, D., 2010: A water-depth correction algorithm for submerged vegetation spectra, Remote Sensing Letters, 1, 29–35, doi:DOI 10.1080/01431160903246709.

Chow, T. V.: Open channel hydraulics, McGraw-Hill Book Company, Inc; New York.

Claude, N., Rodrigues, S., Bustillo, V., Bréhéret, J.-G., Macaire, J.-J., and Jugé, P., 2012: Estimating bedload transport in a large sand–gravel bed river from direct sampling, dune tracking and empirical formulas, Geomorphology, 179, 40–57.

Cobby, D. M., Mason, D. C., and Davenport, I. J., 2001: Image processing of airborne scanning laser altimetry data for improved river flood modelling, ISPRS Journal of Photogrammetry and Remote Sensing, 56, 121–138.

Costa, J., Spicer, K., Cheng, R., Haeni, P., Melcher, N., Thurman, E., Plant, W., and Keller, W., 2000: Measuring stream discharge by non-contact methods: A proof-of-concept experiment, Geophysical Research Letters, 27, 553–556.

David, G. C., Legleiter, C. J., Wohl, E., and Yochum, S. E., 2013: Characterizing spatial variability in velocity and turbulence intensity using 3-D acoustic Doppler velocimeter data in a plane-bed reach of East St. Louis Creek, Colorado, USA, Geomorphology, 183, 28–44.

De Moustier, C. and Matsumoto, H., 1993: Seafloor acoustic remote sensing with multibeam echo-sounders and bathymetric sidescan sonar systems, Marine Geophysical Researches, 15, 27–42.

Dekker, A., Hoogenboom, H., Goddijn, L., and Malthus, T., 1997: The relation between inherent optical properties and reflectance spectra in turbid inland waters, Remote Sensing Reviews, 15, 59–74.

Delai, F., Moretto, J., Picco, L., Rigon, E., Ravazzolo, D., and Lenzi, M., 2014: Analysis of morphological processes in a disturbed gravel-bed river (Piave River): integration of LiDAR data and colour bathymetry, Journal of Civil Engineering and Architecture, 8, 639–648.

Dierssen, H. and Theberge, A., in press: Bathymetry: History of Seafloor Mapping. Encyclopedia of Natural Resources, Taylor & Francis Group. New York.

Dietrich, W. E. and Smith, J. D., 1983: Influence of the point bar on flow through curved channels, Water Resources Research, 19, 1173–1192, doi:10.1029/WR019i005p01173.

Dinehart, R. L. and Burau, J. R., 2005a: Averaged indicators of secondary flow in repeated acoustic Doppler current profiler crossings of bends, Water Resources Research, 41, doi:10.1029/2005WR004050.

Dinehart, R. L. and Burau, J. R., 2005b: Repeated surveys by acoustic Doppler current profiler for flow and sediment dynamics in a tidal river, Journal of Hydrology, 314, 1–21, doi:10.1016/j.hydrol.2005.03.019.

Doxani, G., Papadopoulou, M., Lafazani, P., Pikridas, C., and Tsakiri-Strati, M., 2012: Shallow-Water Bathymetry Over Variable Bottom Types Using Multispectral WORLDVIEW-2 Image, ISPRS-International Archives of the Photogrammetry, Remote Sensing and Spatial Information Sciences, 1, 159–164.

Dufour, S., Bernez, I., Betbeder, J., Corgne, S., Hubert-Moy, L., Nabucet, J., Rapinel, S., Sawtschuk, J., and Trollé, C., 2013: Monitoring restored riparian vegetation: how can recent developments in remote sensing sciences help?, Knowledge and Management of Aquatic Ecosystems, p. 10.

Dury, G., 1967: Some channel characteristics of the Hawkesbury River, New South Wales, Australian Geographical Studies, 5, 135–149.

Dury, G., 1970: A Re-Survey of Part of The Hawkesbury River, New South Wales, After One Hundred Years, Australian Geographical Studies, 8, 121–132.

Entwistle, N. S. and Fuller, I. C.: Terrestrial laser scanning to derive the surface grain size facies character of gravel bars, pp. 102–114, Wiley-Blackwell, doi:10.1002/9781444311952.ch7.

European Commission, 2000: Directive 2000/60/ECC, Establishing a framework for Community action in the field of water policy, Official Journal of the European Communities, L327, 1–71.

Fitzpatrick, C., 2011: SonTek releases the new SonTek-IQ irrigation flow meter, Water21 - magazine of the International Water Association, http://iwapublishing.com/template.cfm?name=w21prodnews111212d.

Fitzpatrick, C., 2012: Remote-control boat speeds reservoir surveys, Water21 - magazine of the International Water Association, http://iwapublishing.com/template.cfm?name=w21prodnews111212d.

Fonstad, M. and Marcus, W., 2005: Remote sensing of stream depths with hydraulically assisted bathymetry (HAB) models, Geomorphology, 72, 320–339, doi:DOI 10.1016/j.geomorph.2005.06.005.

Fonstad, M. A., Dietrich, J. T., Courville, B. C., Jensen, J. L., and Carbonneau, P. E., 2013: Topographic structure from motion: a new development in photogrammetric measurement, Earth Surface Processes and Landforms.

Fox, R.: A. McDonald Introduction to fluid mechanics, New York, John Wiley & Sons.

Frothingham, K. M. and Rhoads, B. L., 2003: Three-dimensional flow structure and channel change in an asymmetrical compound meander loop, Embarras River, Illinois, Earth Surface Processes and Landforms, 28, 625–644, doi:10.1002/esp.471.

Fryer, J. and Kniest, H., 1985: Errors in Depth Determination Caused by Waves in Through-Water Photogrammetry, The Photogrammetric Record, 11, 745–753.

Fuller, I. and Basher, L., 2013: Riverbed digital elevation models as a tool for holistic river management: Motueka River, Nelson, New Zealand, River Research and Applications, 29, 619–633.

Fuller, I. C. and Hutchinson, E. L., 2007: Sediment flux in a small gravel-bed stream: Response to channel remediation works, New Zealand Geographer, 63, 169–180.

Fuller, I. C., Large, A. R., and Milan, D. J., 2003: Quantifying channel development and sediment transfer following chute cutoff in a wandering gravel-bed river, Geomorphology, 54, 307–323.

Gelfenbaum, G., MacMahan, J., and Reniers, A., 2013: Field and Numerical Study of the Columbia River Mouth, Tech. rep., DTIC Document.

Gilvear, D. and Bryant, R.: Analysis of Aerial Photography and Other Remotely Sensed Data, pp. 135–170, John Wiley & Sons, Ltd, doi:10.1002/0470868333.ch6.

Gilvear, D., Hunter, P., and Higgins, T., 2007: An experimental approach to the measurement of the effects of water depth and substrate on optical and near infra-red reflectance: a field-based assessment of the feasibility of mapping submerged in-stream habitat, International Journal of Remote Sensing, 28, 2241–2256, doi:DOI 10.1080/01431160600976079.

Gilvear, D. J., Davids, C., and Tyler, A. N., 2004: The use of remotely sensed data to detect channel hydromorphology; River Tummel, Scotland, River Research and Applications, 20, 795–811.

Glennie, C., Brooks, B., Ericksen, T., Hauser, D., Hudnut, K., Foster, J., and Avery, J., 2013: Compact multipurpose mobile laser scanning system—Initial tests and results, Remote Sensing, 5, 521–538.

Gordon, R. L., 1989: Acoustic Measurement of River Discharge, J. Hydraul. Eng, 115, 925–936, doi:10.1061/(ASCE)0733-9429(1989)115:7(925).

Gould, R. and Arnone, R., 1997: Remote sensing estimates of inherent optical properties in a coastal environment, Remote Sensing of Environment, 61, 290–301.

Guerrero, M. and Lamberti, A., 2011: Flow field and morphology mapping using ADCP and multibeam techniques: Survey in the Po River, Journal of Hydraulic Engineering, 137, 1576–1587, doi:10.1061/(ASCE)HY.1943-7900.0000464.

Gunawan, B., Neary, V. S., and McNutt, J., 2011: ORNL ADV post-processing guide and MATLAB algorithms for MHK site flow and turbulence analysis, ORNL/TML-2011/338, September.

Hakala, T., Suomalainen, J., Kaasalainen, S., and Chen, Y., 2012: Full waveform hyperspectral LiDAR for terrestrial laser scanning, Optics express, 20, 7119–7127.

Hardy, R., Bates, P., and Anderson, M., 1999: The importance of spatial resolution in hydraulic models for floodplain environments, Journal of Hydrology, 216, 124–136.

Hardy, T., 1998: The future of habitat modeling and instream flow assessment techniques, Regulated Rivers-Research & Management, 14, 405–420.

Heritage, G. L. and Milan, D. J., 2009: Terrestrial Laser Scanning of grain roughness in a gravel-bed river, Geomorphology, 113, 4–11, doi:DOI 10.1016/j.geomorph.2009.03.021.

Herlevi, A., 2002: Inherent And Apparent Optical Properties In Relation To Water Quality In Nordic Waters, Ph.D. thesis, University of Helsinki, Report Series In Geophysics, No 45.

Hill, G., Maddock, I., and Bickerton, M., 2008: River habitat mapping: are surface flow type habitats biologically distinct?, in BHS 10th National Hydrology Symposium, Exeter.

Hofmann-Wellenhof, B., Lichtenegger, H., and Wasle, E.: GNSS–global navigation satellite systems: GPS, GLONASS, Galileo, and more, Springer.

Hohenthal, J., Alho, P., Hyyppä, J., and Hyyppä, H., 2011: Laser scanning applications in fluvial studies, Progress in Physical Geography, 35, 782–809.

Hoitink, A., Buschman, F., and Vermeulen, B., 2009: Continuous measurements of discharge from a horizontal acoustic Doppler current profiler in a tidal river, Water resources research, 45.

Holden, H. and LeDrew, E., 2002: Measuring and modeling water column effects on hyperspectral reflectance in a coral reef environment, Remote Sensing of Environment, 81, 300–308, doi:PII S0034-4257(02)00007-X.

Horritt, M., Bates, P., and Mattinson, M., 2006: Effects of mesh resolution and topographic representation in 2D finite volume models of shallow water fluvial flow, Journal of Hydrology, 329, 306–314.

Jaakkola, A., Hyyppa, J., Kukko, A., Yu, X., Kaartinen, H., Lehtomaki, M., and Lin, Y., 2010: A low-cost multi-sensoral mobile mapping system and its feasibility for tree measurements, Isprs Journal of Photogrammetry and Remote Sensing, 65, 514–522, doi:10.1016/j.isprsjprs.2010.08.002.

Jamieson, E., Rennie, C., Jacobson, R., and Townsend, R., 2011: 3-D flow and scour near a submerged wing dike: ADCP measurements on the Missouri River, Water Resources Research, 47, doi:10.1029/2010WR010043.

Jarrett, R. D., 1984: Hydraulics of high-gradient streams, Journal of Hydraulic Engineering, 110, 1519–1539, doi:10.1061/(ASCE)0733-9429(1984)110:11(1519).

Javernick, L., Brasington, J., and Caruso, B., 2014: Modeling the topography of shallow braided rivers using Structure-from-Motion photogrammetry, Geomorphology, 213, 166 – 182, doi:http://dx.doi.org/10.1016/j.geomorph.2014.01.006.

Jordan, D. C. and Fonstad, M. A., 2005: Two Dimensional Mapping of River Bathymetry and Power Using Aerial Photography and GIS on the Brazos River, Texas, GEOCARTO INTERNATIONAL, 20, 13–20.

Kaeser, A. J., Litts, T. L., and Tracy, T. W., 2013: Using Low-Cost Side-Scan Sonar For Benthic Mapping Throughout The Lower Flint River, Georgia, USA, River Research and Applications, 29, 634–644, doi:10.1002/rra.2556.

Kasvi, E., Vaaja, M., Alho, P., Hyyppä, H., Hyyppä, J., Kaartinen, H., and Kukko, A., 2012: Morphological changes on meander point bars associated with flow structure at different discharges, Earth Surface Processes and Landforms, doi:10.1002/esp.3303.

Kasvi, E., Alho, P., Vaaja, M., Hyyppä, H., and Hyyppä, J., 2013: Spatial and temporal distribution of fluvio-morphological processes on a meander point bar during a flood event, Hydrology Research, 44, 1022 – 1039, doi:10.2166/nh.2013.091.

Kasvi, E., Alho, P., Lotsari, E., Wang, Y., Kukko, A., Hyyppä, H., and Hyyppä, J., 2014: Two-dimensional and three-dimensional computational models in hydrodynamic and morphodynamic reconstructions of a river bend: sensitivity and functionality, Hydrological Processes.

Kasvi, E., Vaaja, M., Kaartinen, H., Kukko, A., Jaakkola, A., Flener, C., Hyyppä, H., Hyyppä, J., and Alho, P., 2015: Sub-bend scale flow–sediment interaction of meander bends—A combined approach of field observations, close-range remote sensing and computational modelling, Geomorphology, 238, 119–134.

Kim, D. and Muste, M., 2012: Multi-dimensional representation of river hydrodynamics using ADCP data processing software, Environmental Modelling & Software, 38, 158–166, doi:10.1016/j.envsoft.2012.05.011.

Kinzel, P. J., Legleiter, C. J., and Nelson, J. M., 2013: Mapping River Bathymetry With a Small Footprint Green LiDAR: Applications and Challenges1, Journal Of The American Water Resources Association.

Kiss, T. and Sipos, G., 2007: Braid-scale channel geometry changes in a sand-bedded river: Significance of low stages, Geomorphology, 84, 209–221.

Knighton, D.: Fluvial forms and processes: a new perspective, Routledge.

Kohler, D. D. R. and Philpot, W. D., 1998: Derivative Based Hyperspectral Algorithms for Bathymetric Mapping, in Ocean Optics XIV Conference Kailua-Kona, Hawaii.

Kolev, N. Z., ed., 2011: Sonar systems, InTech.

Koljonen, S.: Ecological Impacts of In-stream Restoration in Salmonid Rivers: The Role of Enhanced Structural Complexity, no. 580 in Acta Universitatis Ouluensis: Scientiae Rerum Naturalium, University of Oulu.

Koljonen, S., Huusko, A., Mäki-Petäys, A., Louhi, P., and Muotka, T., 2012: Assessing Habitat Suitability for Juvenile Atlantic Salmon in Relation to In-Stream Restoration and Discharge Variability, Restoration Ecology, 21, 344–352.

Kondolf, G. M., Boulton, A. J., O'Daniel, S., Poole, G. C., Rachel, F. J., Stanley, E. H., Wohl, E., Bang, A., Carlstrom, J., Cristoni, C., Huber, H., Koljonen, S., Louhi, P., and Nakamura, K., 2006: Process-based ecological river restoration: Visualizing three-dimensional connectivity and dynamic vectors to recover lost linkages, Ecology and Society, 11.

Koponen, S., 2006: Remote sensing of water quality for Finnish lakes and coastal areas, Ph.D. thesis, Helsinki University of Technology, Laboratory of Space Technology, P.O.Box 3000, FIN-02015 HUT, Finland.

Kostaschuk, R., Best, J., Villard, P., Peakall, J., and Franklin, M., 2005: Measuring flow velocity and sediment transport with an acoustic Doppler current profiler, Geomorphology, 68, 25–37, doi:10.1016/j.geomorph.2004.07.01.

Kostylev, V., Todd, B., Fader, G., Courtney, R., Cameron, G., and Pickrill, R., 2001: Benthic habitat mapping on the Scotian Shelf based on multibeam bathymetry, surficial geology and sea floor photographs, Marine Ecology-Progress Series, 219, 121–137.

Kraus, N. C., Lohrmann, A., and Cabrera, R., 1994: New acoustic meter for measuring 3D laboratory flows, Journal of Hydraulic Engineering, 120, 406–412.

Kukko, A., Kaartinen, H., Hyyppä, J., and Chen, Y., 2012: Multiplatform Mobile Laser Scanning: Usability and Performance, Sensors, 12, 11 712–11 733.

Laamanen, L., Flener, C., and Alho, P., 2014: Spatio-temporal flow structures and morphological changes in a meander bend during a spring flood:a unique ADCP mini-boat approach, in Geophysical Research Abstracts, vol. 16 of *Geophysical Research Abstracts*, EGU General Assembly 2014.

Lafon, V., Froidefond, J., Lahet, F., and Castaing, P., 2002: SPOT shallow water bathymetry of a moderately turbid tidal inlet based on field measurements, Remote Sensing of Environment, 81, 136–148, doi:PII S0034-4257(01)00340-6.

Lane, S., Richards, K., and Chandler, J., 1993: Developments in photogrammetry; the geomorphological potential, Progress in Physical Geography, 17, 306–328.

Lane, S., Richards, K., and Chandler, J., 1994: Developments in monitoring and modelling small-scale river bed topography, Earth Surface Processes and Landforms, 19, 349–368.

Lane, S., Biron, P., Bradbrook, K., Butler, J., Chandler, J., Crowell, M., McLelland, S., Richards, K., and Roy, A., 1998: Three-dimensional measurement of river channel flow processes using acoustic Doppler velocimetry, Earth Surface Processes and Landforms, 23, 1247–1267.

Lane, S., Bradbrook, K., Richards, K., Biron, P., and Roy, A., 1999: The application of computational fluid dynamics to natural river channels: three-dimensional versus two-dimensional approaches, Geomorphology, 29, 1–20.

Lane, S., Westaway, R., and Hicks, D., 2003: Estimation of erosion and deposition volumes in a large, gravel-bed, braided river using synoptic remote sensing, Earth Surface Processes and Landforms, 28, 249–271, doi:DOI 10.1002/esp.483.

Lane, S., Widdison, P., Thomas, R., Ashworth, P., Best, J., Lunt, I., Sambrook Smith, G., and Simpson, C., 2010: Quantification of braided river channel change using archival digital image analysis, Earth Surface Processes and Landforms, 35, 971–985.

Lee, Z., Carder, K. L., Mobley, C. D., Steward, R. G., and Patch, J. S., 1999: Hyperspectral Remote Sensing for Shallow Waters. 2. Deriving Bottom Depths and Water Properties by Optimization, Applied Optics, 38, 3831–3843.

Leeder, M., 1983: On the dynamics of sediment suspension by residual Reynolds stresses—confirmation of Bagnold's theory, Sedimentology, 30, 485–491.

Legleiter, C. and Roberts, D., 2005: Effects of channel morphology and sensor spatial resolution on image-derived depth estimates, Remote Sensing of Environment, 95, 231–247, doi:DOI 10.1016/j.rse.2004.12.013.

Legleiter, C., Roberts, D., Marcus, W., and Fonstad, M., 2004: Passive optical remote sensing of river channel morphology and in-stream habitat: Physical basis and feasibility, Remote Sensing of Environment, 93, 493–510, doi:DOI 10.1016/j.rse.2004.07.019.

Legleiter, C., Roberts, D., and Lawrence, R., 2009: Spectrally based remote sensing of river bathymetry, Earth Surface Processes and Landforms, 34, 1039–1059.

Legleiter, C. J., 2003: Spectrally Driven Classification of High Spatial Resolution, Hyperspectral Imagery: A Tool for Mapping In-Stream Habitat, Environmental Management, 32, 399–411, doi:10.1007/s00267-003-0034-1.

Legleiter, C. J. and Fonstad, M. A.: An Introduction to the Physical Basis for Deriving River Information by Optical Remote Sensing, pp. 43–69, John Wiley & Sons, Ltd, doi:10.1002/9781119940791.ch3.

Legleiter, C. J. and Overstreet, B. T., 2012: Mapping gravel bed river bathymetry from space, Journal of Geophysical Research: Earth Surface (2003–2012), 117.

Leopold, L. B., 1953: Downstream change of velocity in rivers, American Journal of Science, 251, 606–624.

Leopold, L. B. and Wolman, M. G., 1960: River meanders, Geological Society of America Bulletin, 71, 769–793.

Liceaga-Correa, M. and Euan-Avila, J., 2002: Assessment of coral reef bathymetric mapping using visible Landsat Thematic Mapper data, International Journal of Remote Sensing, 23, 3–14.

Lillesand, T. M., Kiefer, R. W., and Chipman, J. W.: Remote sensing and image interpretation., Ed. 6, John Wiley & Sons Ltd.

Liu, Y., Islam, M., and Gao, J., 2003: Quantification of shallow water quality parameters by means of remote sensing, doi:DOI 10.1191/0309133303pp357ra, doi:DOI 10.1191/0309133303pp357ra.

Lorang, M., Whited, D., Hauer, F., Kimball, J., and Stanford, J. A., 2005: Using airborne multispectral imagery to evaluate geomorphic work across floodplains of gravel-bed rivers, Ecological Applications, 15, 1209–1222.

Lotsari, E., Veijalainen, N., Alho, P., and Kayhko, J., 2010: Impact of climate change on future discharges and flow characteristics of the Tana river, sub-arctic northern Fennoscandia, Geografiska Annaler Series A-Physical Geography, 92A, 263–284, doi:10.1111/j.1468-0459.2010.00394.x.

Lotsari, E., Wainwright, D., Corner, G., Alho, P., and Käyhkö, J., 2013: Surveyed and modelled one-year morphodynamics in the braided lower Tana River, Hydrological Processes, doi:10.1002/hyp.9750.

Lotsari, E., Vaaja, M., Flener, C., Kaartinen, H., Kukko, A., Kasvi, E., Hyyppä, H., Hyyppä, J., and Alho, P., 2014: Annual bank and point bar morphodynamics of a meandering river determined by high-accuracy multitemporal laser scanning and flow data, Water Resources Research, 50, 5532–5559, doi:10.1002/2013WR014106.

Lundahl, A. C., 1948: Underwater depth determination by aerial photography, Photogrammetric Engineering, 14, 454–462.

Lyon, J., Lunetta, R., and Williams, D., 1992: Airborne multispectral scanner data for evaluating bottom sediment types and water depths of the St Marys river, Michigan, Photogrammetric Engineering and Remote Sensing, 58, 951–956.

Lyzenga, D. R., 1981: Remote sensing of bottom reflectance and water attenuation parameters in shallow water using aircraft and Landsat data, International Journal of Remote Sensing, 2, 71 – 82, doi:10.1080/01431168108948342.

Lyzenga, D. R., Malinas, N. R., and Tanis, F. J., 2006: Multispectral bathymetry using a simple physically based algorithm, Ieee Transactions On Geoscience and Remote Sensing, 44, 2251–2259, doi:DOI 10.1109/TGRS.2006.872909.

Mandlburger, G. and Brockmann, H., 2001: Modelling a watercourse DTM based on airborne laser-scanner data, in OEEPE Workshop on Airborne Laserscanning and Interferometric SAR for Detailed Digital Elevation Models, Official Publication, 40, pp. 111–120.

Manley, P. and Singer, J., 2008: Assessment of sedimentation processes determined from side-scan sonar surveys in the Buffalo River, New York, USA, Environmental geology, 55, 1587–1599.

Mansikkaniemi, H., 1972: Flood deposits, transport distancies and roundness of loose material in the Tana river valley, Lapland, Turun yliopiston julkaisuja. Sarja A. II. Biologica - Geographica - Geologica, 49, 15–23.

Mansikkaniemi, H. and Mäki, O.-P., 1990: Palaeochannels and recent changes in the Pulmankijoki valley, northern Lapland, Fennia, 168, 137–152.

Manu, L., Tsukamoto, T., Nakanishi, K., Lina, L., Shirozu, H., Hokamura, T., and Yamada, F., 2014: The Effects of Flooding on Shirakawa Delta Morphology.

Marcus, W., Legleiter, C., Aspinall, R., Boardman, J., and Crabtree, R., 2003: High spatial resolution hyperspectral mapping of in-stream habitats, depths, and woody debris in mountain streams, Geomorphology, 55, 363–380, doi:DOI 10.1016/S0169-555X(03)00150-8.

Marcus, W. A., 2002: Mapping of stream microhabitats with high spatial resolution hyperspectral imagery., Journal of Geographical Systems, 4, p113 –.

Marcus, W. A. and Fonstad, M. A., 2008: Optical remote mapping of rivers at sub-meter resolutions and watershed extents, Earth Surface Processes and Landforms, 33, 4–24.

Marcus, W. A. and Fonstad, M. A., 2010: Remote sensing of rivers: the emergence of a subdiscipline in the river sciences, Earth Surface Processes and Landforms, 35, 1867–1872, doi:10.1002/esp.2094.

Marcus, W. A., Fonstad, M. A., and Legleiter, C. J.: Management Applications of Optical Remote Sensing in the Active River Channel, pp. 19–41, John Wiley & Sons, Ltd, doi:10.1002/9781119940791.ch2.

Maxwell, S. L. and Smith, A. V., 2007: Generating River Bottom Profiles with a Dual-Frequency Identification Sonar (DIDSON), North American Journal of Fisheries Management, 27, 1294–1309, doi:10.1577/M07-019.1.

Mertes, L., 2002: Remote sensing of riverine landscapes, Freshwater Biology, 47, 799–816.

Mertes, L. A., Smith, M. O., and Adams, J. B., 1993: Estimating suspended sediment concentrations in surface waters of the Amazon River wetlands from Landsat images, Remote Sensing of Environment, 43, 281–301.

Merwade, V., 2009: Effect of spatial trends on interpolation of river bathymetry, Journal of Hydrology, 371, 169–181.

Micheletti, N., Chandler, J. H., and Lane, S. N., 2014: Investigating the geomorphological potential of freely available and accessible structure-from-motion photogrammetry using a smartphone, Earth Surface Processes and Landforms.

Milan, D. J., Heritage, G. L., and Hetherington, D., 2007: Application of a 3D laser scanner in the assessment of erosion and deposition volumes and channel change in a proglacial river, Earth surface processes and landforms, 32, 1657–1674.

Milan, D. J., Heritage, G. L., Large, A. R. G., and Fuller, I. C., 2011: Filtering spatial error from DEMs: Implications for morphological change estimation, Geomorphology, 125, 160–171, doi:DOI 10.1016/j.geomorph.2010.09.012.

Milne, J. A. and Sear, D. A., 1997: Modelling river channel topography using GIS, International Journal of Geographical Information Science, 11, 499 – 519.

Möller, T. J., Holfort, J., Delahoyde, F., and Williams, R., 1995: MKIIIB-CTD: improving its system output, Deep Sea Research Part I: Oceanographic Research Papers, 42, 2113–2126.

Moretto, J., Rigon, E., Mao, L., Delai, F., Picco, L., and Lenzi, M., 2012: Assessing morphological changes in gravel-bed rivers using LiDAR data and colour bathymetry, IAHS-AISH publication, pp. 419–427.

Moretto, J., Delai, F., Picco, L., and Lenzi, M. A., 2013: Integration of colour bathymetry, LiDAR and dGPS surveys for assessing fluvial changes after flood events in the Tagliamento River (Italy), Agricultural Sciences, 2013.

Morris, T., 2009: Lecture material: Elements of ecology, Fullerton College, http://www.seos-project.eu/modules/oceancolour/oceancolour-c01-p07.html.

Mueller, D., Abad, J., García, C., Gartner, J., García, M., and Oberg, K., 2007: Errors in Acoustic Doppler Profiler Velocity Measurements Caused by Flow Disturbance, Journal of Hydraulic Engineering, 133, 1411–1420, doi:10.1061/(ASCE)0733-9429(2007)133:12(1411).

Murase, T., Tanaka, M., Tani, T., Miyashita, Y., Ohkawa, N., Ishiguro, S., Suzuki, Y., Kayanne, H., and Yamano, H., 2008: A photogrammetric correction procedure for light refraction effects at a two-medium boundary, Photogrammetric Engineering & Remote Sensing, 74, 1129–1136.

Muste, M., Yu, K., Pratt, T., and Abraham, D., 2004a: Practical aspects of ADCP data use for quantification of mean river flow characteristics; Part II: fixed-vessel measurements, Flow Measurement and Instrumentation, 15, 17–28, doi:10.1016/j.flowmeasinst.2003.09.002.

Muste, M., Yu, K., and Spasojevic, M., 2004b: Practical aspects of ADCP data use for quantification of mean river flow characteristics; Part I: moving-vessel measurements, Flow measurement and instrumentation, 15, 1–16, doi:10.1016/j.flowmeasinst.2003.09.001.

Muste, M., Kim, D., and González-Castro, J. A., 2009: Near-transducer errors in ADCP measurements: experimental findings, Journal of Hydraulic Engineering, 136, 275–289.

Nanson, R. A., 2010: Flow fields in tightly curving meander bends of low width-depth ratio, Earth Surface Processes and Landforms, 35, 119–135.

Nihei, Y. and Kimizu, A., 2008: A new monitoring system for river discharge with horizontal acoustic Doppler current profiler measurements and river flow simulation, Water resources research, 44.

Nystrom, E., Rehmann, C., and Oberg, K., 2007: Evaluation of Mean Velocity and Turbulence Measurements with ADCPs, Journal of Hydraulic Engineering, 133, 1310–1318, doi:10.1061/(ASCE)0733-9429(2007)133:12(1310).

Oksanen, J., 2006: Digital Elevation Model Error in Terrain Analysis, Doctoral dissertation, University of Helsinki, Faculty of Science, Department of Geography and Finnish Geodetic Institute, Department of Geoinformatics and Cartography, Finnish Geodetic Institute P.O.Box 15, FI-02431 Masala, Finland.

Papa, F., Prigent, C., and Rossow, W. B., 2007: Ob' river flood inundations from satellite observations: A relationship with winter snow parameters and river runoff, Journal of Geophysical Research-Atmospheres, 112, D18 103.

Parsons, D., Best, J., Orfeo, O., Hardy, R., Kostaschuk, R., and Lane, S., 2005: Morphology and flow fields of three-dimensional dunes, Rio Paraná, Argentina: Results from simultaneous multibeam echo sounding and acoustic Doppler current profiling, Journal of Geophysical Research: Earth Surface (2003–2012), 110.

Parsons, D., Jackson, P., Czuba, J., Engel, F., Rhoads, B., Oberg, K., Best, J., Mueller, D., Johnson, K., and Riley, J., 2013: Velocity Mapping Toolbox (VMT): a processing and visualization suite for moving-vessel ADCP measurements, Earth Surface Processes and Landforms.

Patterson, J., Bushnell, M., and Haenggi, M., 2011: A field evaluation of the CastAway CTD at the Deepwater Horizon Oil spill site in the gulf of Mexico, in OCEANS 2011, pp. 1–9, IEEE.

Petrie, J., Diplas, P., Gutierrez, M., and Nam, S., 2013: Combining fixed-and moving-vessel acoustic Doppler current profiler measurements for improved characterization of the mean flow in a natural river, Water Resources Research, 49, 5600–5614.

Pyle, C., Richards, K., and Chandler, J., 1997: Digital photogrammetric monitoring of river bank erosion, The Photogrammetric Record, 15, 753–764.

R Development Core Team, 2008: R: A Language and Environment for Statistical Computing, R Foundation for Statistical Computing, Vienna, Austria, http://www.R-project.org.

Ramooz, R. and Rennie, C. D., 2010: Laboratory Measurement of Bedload with an ADCP, U.S. Geological Survey Scientific Investigations Report 2010-5091, pp. 367–386.

Rehmel, M., 2007: Application of Acoustic Doppler Velocimeters for Streamflow Measurements, Journal of Hydraulic Engineering, 133, 1433–1438, doi:10.1061/(ASCE)0733-9429(2007)133:12(1433).

Rennie, C. D., 2008: Uncertainty of ADCP spatial velocity distributions, in 6th International Symposium on ultrasonic doppler method for fluid mechanics and fluid engineering, Prague, Czech republic.

Rennie, C. D. and Church, M., 2010: Mapping spatial distributions and uncertainty of water and sediment flux in a large gravel bed river reach using an acoustic Doppler current profiler, Journal of Geophysical Research: Earth Surface (2003–2012), 115.

Rennie, C. D. and Rainville, F., 2006: Case study of precision of GPS differential correction strategies: Influence on aDcp velocity and discharge estimates, Journal of hydraulic engineering, 132, 225–234, doi:10.1061/(ASCE)0733-9429(2006)132:3(225).

Reynolds, O., 1883: An experimental investigation of the circumstances which determine whether the motion of water shall be direct or sinuous, and of the law of resistance in parallel channels., Proceedings of the royal society of London, 35, 84–99.

Robert, A. et al.: River processes: an introduction to fluvial dynamics., Routledge.

Roberts, A. and Anderson, J., 1999: Shallow water bathymetry using integrated airborne multi-spectral remote sensing, International Journal of Remote Sensing, 20, 497–510.

Rogala, J. T., 1999: Upper Mississippi River System Navigation Feasibility Study. Interim Report for the Upper Mississippi River – Illinois Waterway System Navigation Study, ENV Report 13, U.S. Army Engineers District, Rock Island, U.S. Army Engineers District, St. Louis, and U.S. Army Engineers District, St. Paul.

Saarinen, N., Vastaranta, M., Vaaja, M., Lotsari, E., Jaakkola, A., Kukko, A., Kaartinen, H., Holopainen, M., Hyyppä, H., and Alho, P., 2013: Area-Based Approach for Mapping and Monitoring Riverine Vegetation Using Mobile Laser Scanning, Remote Sensing, 5, 5285–5303.

Sagawa, T., Komatsu, T., Boisnier, E., Mustapha, K. B., Hattour, A., Kosaka, N., and Miyazaki, S., 2007: A New Applicaton Method for Lyzenga's Optical Model, in Proceedings of the 2007 Annual Conference of the Remote Sensing & Photogrammetry Society (RSPSoc2007), Newcastle upon Tyne.

Sandidge, J. and Holyer, R., 1998: Coastal bathymetry from hyperspectral observations of water radiance, Remote Sensing of Environment, 65, 341–352.

Schäppi, B., Perona, P., Schneider, P., and Burlando, P., 2010: Integrating river cross section measurements with digital terrain models for improved flow modelling applications, Computers & Geosciences, 36, 707–716.

Schmidtlein, S., 2005: Imaging spectroscopy as a tool for mapping Ellenberg indicator values, Journal of Applied Ecology, 42, 966–974, doi:DOI 10.1111/j.1365-2664.2005.01064.x.

Shields, F. and Rigby, J., 2005: River habitat quality from river velocities measured using acoustic Doppler current profiler, Environmental Management, 36, 565–575, doi:DOI 10.1007/s00267-004-0292-6.

Shields, F. D., Knight, S. S., Cooper, C. M., et al., 2003: Use of acoustic Doppler current profilers to describe velocity distributions at the reach scale, JAWRA Journal of the American Water Resources Association, 39, 1397–1408, doi:10.1111/j.1752-1688.2003.tb04426.x.

Simpson, J., Mitchelson-Jacob, E., and Hill, A., 1990: Flow structure in a channel from an acoustic Doppler current profiler, Continental Shelf Research, 10, 589–603.

Simpson, M. R., 2001: Discharge measurements using a broad-band acoustic Doppler current profiler, Open-file report 01-1, US Geological Survey, Sacramento, California.

Sirniö, V.-P., 2004: Uoman Kartoitus -Teknologia, Maankäyttö, 3.

Smith, L. C., 1997: Satellite remote sensing of river inundation area, stage, and discharge: A review, Hydrological processes, 11, 1427–1439.

Smith, M. and Pain, C., 2009: Applications of remote sensing in geomorphology, Progress in Physical Geography, 33, 568–582.

Smith, M., Vericat, D., and Gibbins, C., 2012: Through-water terrestrial laser scanning of gravel beds at the patch scale, Earth Surface Processes and Landforms, 37, 411–421.

Smith, M. J., Chandler, J., and Rose, J., 2009: High spatial resolution data acquisition for the geosciences: kite aerial photography, Earth Surface Processes and Landforms, 34, 155–161.

Stumpf, R. P., Holderied, K., Robinson, J. A., Feldman, G., and Kuring, N., 2003: Mapping Water Depths in Clear Water From Space, in Proceedings of the 13th Biennial Coastal Zone Conference.

Sukhodolov, A. N., 2012: Structure of turbulent flow in a meander bend of a lowland river, Water Resources Research, 48, doi:10.1029/2011WR010765.

Tamminga, A., Hugenholtz, C., Eaton, B., and Lapointe, M., 2014: Hyperspatial Remote Sensing Of Channel Reach Morphology And Hydraulic Fish Habitat Using An Unmanned Aerial Vehicle (UAV): A First Assessment In The Context Of River Research And Management, River Research and Applications.

Tetis, U. M. R., 2010: Geostatistical estimations of bathymetric LiDAR errors on rivers, Earth, 1210, 1199–1210, doi:10.1002/esp.1991.

Tsubaki, R., Kawahara, Y., Muto, Y., and Fujita, I., 2012: New 3-D flow interpolation method on moving ADCP data, Water Resources Research, 48.

Vaaja, M., Hyyppä, J., Kukko, A., Kaartinen, H., Hyyppä, H., and Alho, P., 2011a: Mapping topography changes and elevation accuracies using a mobile laser scanner, Remote Sensing, 3, 587–600.

Vaaja, M., Kurkela, M., Hyyppä, H., Alho, P., Hyyppä, J., Kukko, A., Kaartinen, H., Kasvi, E., Kaasalainen, S., and Rönnholm, P., 2011b: Fusion of Mobile Laser Scanning and Panoramic Images for Studying River Environment Topography and Changes, ISPRS-International Archives of the Photogrammetry, Remote Sensing and Spatial Information Sciences, 3812, 319–324.

Vaaja, M., Kukko, A., Kaartinen, H., Kurkela, M., Kasvi, E., Flener, C., Hyyppä, H., Hyyppä, J., Järvelä, J., and Alho, P., 2013: Data Processing and Quality Evaluation of a Boat-Based Mobile Laser Scanning System, Sensors, 13, 12 497–12 515, doi:10.3390/s130912497.

Vaughan, I., Diamond, M., Gurnell, A., Hall, K., Jenkins, A., Milner, N., Naylor, L., Sear, D., Woodward, G., and Ormerod, S., 2009: Integrating ecology with hydromorphology: a priority for river science and management, Aquatic Conservation: Marine and Freshwater Ecosystems, 19, 113–125.

Vericat, D., Narciso, E., Béjar, M., Tena, Á., Brasington, J., Gibbins, C., and Batalla, R. J., 2014: From the air to digital landscapes: generating reach-scale topographic models from aerial photography in gravel-bed rivers, in EGU General Assembly Conference Abstracts, vol. 16, p. 9411.

Vetter, M., Hofle, B., Mandlburger, G., and Rutzinger, M., 2011: Estimating changes of riverine landscapes and riverbeds by using airborne LiDAR data and river cross-sections, Zeitschrift für Geomorphologie, Supplementary Issues, 55, 51–65.

Virtanen, M., Koponen, J., Hellsten, S., Nenonen, O., and Kinnunen, K., 1994: Principles for calculation of transport and water quality in strongly regulated reservoirs, Ecological modelling, 74, 103–123.

Wagner, C. R. and Mueller, D. S., 2011: Comparison of bottom-track to global positioning system referenced discharges measured using an acoustic Doppler current profiler, Journal of Hydrology, 401, 250–258.

Wagner, W., Ullrich, A., Melzer, T., Briese, C., and Kraus, K., 2004: From Single-Pulse to Full-Waveform Airborne Laser Scanners: Potential and Practical Challenges, International Archives of Photogrammetry and Remote Sensing, XXXV, 201–206.

Walther, S. C., Marcus, W. A., and Fonstad, M. A., 2011: Evaluation of high-resolution, true-colour, aerial imagery for mapping bathymetry in a clear-water river without ground-based depth measurements, International Journal of Remote Sensing, 32, 4343–4363.

Wang, Y., Liang, X., Flener, C., Kukko, A., Kaartinen, H., Kurkela, M., Vaaja, M., Hyyppä, H., and Alho, P., 2013: 3D Modeling of Coarse Fluvial Sediments Based on Mobile Laser Scanning Data, Remote Sensing, 5, 4571–4592, doi:10.3390/rs5094571.

Westaway, R. M., Lane, S. N., and Hicks, D. M., 2001: Remote sensing of clear-water, shallow, gravel-bed rivers using digital photogrammetry, Photogrammetric Engineering and Remote Sensing, 67, 1271–1282.

Westaway, R. M., Lane, S. N., and Hicks, D. M., 2003: Remote survey of large-scale braided, gravel-bed rivers using digital photogrammetry and image analysis, International Journal of Remote Sensing, 24, 795–815, doi:DOI 10.1080/01431160110113070.

Wheaton, J. M., Brasington, J., Darby, S. E., Merz, J., Pasternack, G. B., Sear, D., and Vericat, D., 2010: Linking geomorphic changes to salmonid habitat at a scale relevant to fish, River Research and Applications, 26, 469–486.

White, L. and Hodges, B. R., 2005: Filtering the signature of submerged large woody debris from bathymetry data, Journal of Hydrology, 309, 53–65.

Williams, R., Brasington, J., Vericat, D., Hicks, M., Labrosse, F., and Neal, M., 2011: Monitoring Braided River Change Using Terrestrial Laser Scanning and Optical Bathymetric Mapping, in Geomorphological Mapping Methods and Applications, edited by P. P. Mike J. Smith and J. S. Griffiths, vol. 15 of *Developments in Earth Surface Processes*, chap. 20, pp. 507 – 532, Elsevier, doi:10.1016/B978-0-444-53446-0.00020-3.

Williams, R., Brasington, J., Vericat, D., and Hicks, D., 2013a: Hyperscale terrain modelling of braided rivers: fusing mobile terrestrial laser scanning and optical bathymetric mapping, Earth Surface Processes and Landforms, doi:10.1002/esp.3437.

Williams, R., Rennie, C., Brasington, J., Hicks, D., and Vericat, D., 2015: Linking the spatial distribution of bedload transport to morphological change during high-flow events in a shallow braided river, Journal of Geophysical Research: Earth Surface, pp. http–dx, doi:10.1002/2014JF003346.

Williams, R. D., Brasington, J., Hicks, M., Measures, R., Rennie, C., and Vericat, D., 2013b: Hydraulic validation of two-dimensional simulations of braided river flow with spatially continuous aDcp data, Water Resources Research, 49, 5183–5205, doi:10.1002/wrcr.20391.

Winterbottom, S. J. and Gilvear, D. J., 1997: Quantification of channel bed morphology in gravel-bed rivers using airborne multispectral imagery and aerial photography, Regulated Rivers-Research & Management, 13, 489–499.

WMO, 2008: Guide to Hydrological Practices (WMO No.168) Volume I: Hydrology – From Measurement to Hydrological Information, World Meteorological Organization (WMO), Geneva, Switzerland.

Wohl, E.: Rivers in the Landscape: Science and Management, Wiley-Blackwell.

Wohl, E. E., 1998: Uncertainty in flood estimates associated with roughness coefficient, Journal of Hydraulic Engineering, 124, 219–223.

Wright, A., Marcus, W., and Aspinall, R., 2000: Evaluation of multispectral, fine scale digital imagery as a tool for mapping stream morphology, Geomorphology, 33, 107–120.

Yorke, T. H. and Oberg, K. A., 2002: Measuring river velocity and discharge with acoustic Doppler profilers, Flow Measurement and Instrumentation, 13, 191–195.

Zhao, J., Chen, Z., and Zhang, H., 2014: A robust method for determining the heading misalignment angle of GPS compass in ADCP measurement, Flow Measurement and Instrumentation, 35, 1–10, doi:10.1016/j.flowmeasinst.2013.10.005.

Zinke, P. and Flener, C., 2013: Experiences from the use of Unmanned Aerial Vehicles (UAV) for River Bathymetry Modelling in Norway, VANN, 48, 351 – 360.